frontiers in Materials

REVIEW
published: 28 October 2021
doi: 10.3389/fmats.2021.754431

Recent Advances in Magnesia Blended Cement Studies for Geotechnical Well Construction—A Review

Weiqing Chen, Salaheldin Elkatatny, Mobeen Murtaza and Ahmed Abdulhamid Mahmoud*

College of Petroleum Engineering & Geosciences, King Fahd University of Petroleum & Minerals (KFUPM), Dhahran, Saudi Arabia

The current paper presents a literature review on the studies of incorporation of magnesia (magnesium oxide) into Portland cement material from the geotechnical well construction perspective. Starting with a comparison of application conditions between civil construction and geotechnical well cementing, this work reviewed the Portland cement categorizations, magnesia manufacturing routes at first. Then, the physical-chemical-mechanical properties were investigated which includes the reactivity of magnesia, expansion influence from its hydration, and carbonation/dehydroxylation of magnesia blended Portland cement. The development of cement material hydration modeling methods is also summarized. Moreover, the experimental characterization methods have also been elucidated including composition determination, particle size analysis, volumetric variation measurement, compressive strength testing, shear-bond strength testing, transition state analysis, etc. Meanwhile, the results and conclusions were extracted from the literature. Through this route, a comprehensive understanding of the scientific research progress on magnesia blended Portland cement development for geotechnical well construction is derived. Additionally, it is concluded that incorporating magnesia into Portland cement can provide benefits for this material utilization in geotechnical well constructions provided the reasonable tuning among the characteristics of magnesia, the downhole surrounding conditions, and the formulation of the cement slurry. Satisfying these pre-conditions, the effective expansion not only mitigates the micro-annulus issues but also increases the shear bonding strength at the cementing interfaces. Moreover, the caustic magnesia introduction into Portland cement has the potential advantage on carbon dioxide geological sequestration well integrity compared with the Portland cement sheath without it because of the denser *in-situ* porous matrix evolvement and more stable carbon fixation features of magnesium carbonate. However, since the impact of magnesia on Portland cement strongly depended on its properties (calcination conditions, particle size, reactivity) and the aging conditions (downhole temperature, pressure, contacting medium), it should be noted that some extended research is worth conducting in the future such as the synchronized hydration between magnesia and Portland cement, the dosage limit of caustic magnesia in Portland cement in terms of CO_2 sequestration and the corresponding mechanical properties analysis, and the hybrid method (caustic magnesia, Portland cement, and other

OPEN ACCESS

Edited by:
Feng Yang,
China University of Geosciences, China

Reviewed by:
Kai Wei,
Yangtze University, China
Huajie Liu,
China University of Petroleum (Huadong), China

***Correspondence:**
Weiqing Chen
jerromychan@gmail.com

Specialty section:
This article was submitted to Structural Materials, a section of the journal Frontiers in Materials

Received: *06 August 2021*
Accepted: *01 October 2021*
Published: *28 October 2021*

Citation:
Chen W, Elkatatny S, Murtaza M and Mahmoud AA (2021) Recent Advances in Magnesia Blended Cement Studies for Geotechnical Well Construction—A Review. Front. Mater. 8:754431. doi: 10.3389/fmats.2021.754431

supplementary cementitious materials) targeting the co-existence of the geothermal environment and the corrosive medium scenario.

Keywords: Portland cement, magnesia, geotechnical well, expansion, shrinkage, hydration, carbonation, well integrity

1 INTRODUCTION

Our modern society is based on the material of cement to some extent, which has been used by humans since at least ten thousand years ago in Neolithic times (Trout, 2019; UNESCO, 2021). At present, cement material has been the most popular binder material (Frederick and Thomas, 2020) globally and has been being developed by humans continuously to satisfy diverse construction requirements.

The first occurrence of magnesia in binder materials application, Sorel cement, can be tracked back to 1867 (Shand, 2006d; Zgueb et al., 2018). Despite some technical advantages like higher compressive strength, better resilience, and quicker early hydration versus Portland cement (PC), the Sorel cement gradually waned in its application because of poor water resistance and magnesium leaching issue (Sorre and Armstrong, 1976; Maravelaki-Kalaitzaki and Moraitou, 1999; Al-Tabbaa, 2013).

Peering on the origin time of Sorel cement, especially compared with the patented origin of PC in 1824 by Joseph Aspin (Biernacki et al., 2017; Frederick and Thomas, 2020), the magnesia blended cement has a similar niche history as PC. However, during the following technical evolution over more than one century, PC paved its dominance among other binder materials (Walling and Provis, 2016).

Nevertheless, compared with civil construction applications, Portland cement has been enduring the probable toughest surroundings in geotechnical wells (oil and gas well, CO_2 sequestration well, and geothermal well) (Michaux et al., 1989). Much higher curing and service temperature and pressure, coupled with more stringent technical requirements such as avoidance of micro-annuli and good bonding strength at cementing interfaces lays the prominent distinguishments of applying the cementitious materials downhole from the civil construction above the ground. Enlightened by the hydration expansion property of magnesia (Thomas J. et al., 2014; Mo et al., 2015; Ye et al., 2015; Temiz et al., 2015; Sherir et al., 2016; Jafariesfad et al., 2016; Qureshi et al., 2016; Sherir et al., 2017; Cao et al., 2018b,a; Srivastava et al., 2018; José et al., 2020; Li et al., 2010; Mo and Al-Tabbaa, 2020) and successful bulk shrinkage prevention case of Baishan dam construction (Mo et al., 2014), incorporating magnesia into Portland cement to address/mitigate its shrinkage issue arouses people's interest rather than simply categorizing magnesia as the detrimental role for the unsoundness of Portland cement application.

To achieve the principal engineering goals of geotechnical wells, zonal isolation and well integrity are the key points which ensure well safety within the different time frames, prevention of environmental issues, and economic longevity of well life (Nelson and Guillot, 2006). Based on this, magnesia presented its application value in this field. Since the intrinsic shrinkage characteristics of Portland cement and the expandable capability of magnesia hydration, magnesia has been studied and applied as one of the expansive additives for several decades. The magnesia-based expandable agent has good thermal stability (Shand, 2006a) and effective expansion under high temperature and high-pressure conditions (Ghofrani and Plack, 1993). This benefits the shrinkage compensation when blending magnesia with Portland cement. In addition to the bulk shrinkage compensation capability, the shear bonding strength at cementing interfaces (between casing and cement sheath, between cement sheath and formation) can also be improved by the induced bulk expansion from magnesia hydration (Ghofrani and Plack, 1993; Rubiandini et al., 2005; Suhascaryo et al., 2005). Meanwhile, because of the *in-situ* magnesium hydroxide crystal growth in the pore matrix of the setting cement, the porosity and permeability of the hardened cement can be impacted based on different confining conditions. If the hardening cement bulk expansion is induced by magnesia hydration under unrestrained conditions, the porosity will probably increase (Ghofrani and Plack, 1993; José et al., 2020). On the contrary, if restrained by external volumetric confining, the expansion probably will favor the sealing capacity with decreasing porosity/permeability (Ghofrani and Plack, 1993; Huajun et al., 2013). Furthermore, magnesia hydration reactivity can be manipulated by its calcination conditions (calcination temperature, residence time) (Mo et al., 2010). Different calcination conditions will produce different particle sizes of magnesia. The curing condition also has a strong impact on the hydration of magnesia (Thomas J. J. et al., 2014). These findings provide us with the high potential to achieve better cement sheath performance corresponding to the downhole conditions.

Apart from addressing the well integrity issues in the petroleum engineering field, the magnesia blended cement also sheds light on the economical and sustainable geotechnical well constructions in respect of environmental protection consciousness (lower energy consumption in the manufacturing process compared with PC's process, CO_2 geological sequestration, and potential carbon neutralization) in recent years. For instance, as for the greenhouse gas issue, the Portland cement manufacturing industry contributes substantial CO_2 emissions annually. The source of CO_2 usually arises from two aspects as 1) inherent chemical reaction regarding limestone calcination around 1,450°C which occupies 4% of the CO_2 global emission (Crippa et al., 2017; Olivier and Peters, 2017), and 2) fuel consumption during the clinker calcination heating process. In recent years, the annual production of Portland cement has arrived at 4 billion metric tons (Curry and van Oss, 2017) which contributes approximately 8–10% of all CO_2 emissions due to human activity (Pearce, 1997; Lehne and Preston, 2017; Rodgers, 2018). On the other hand, the thermal decomposition temperature from minerals to magnesia is much lower than the Portland cement's (as for dolomite and magnesite 550°C–750°C, as for brucite 350°C) (Mitchell, 1923; Shand, 2006c; Liu et al., 2017).

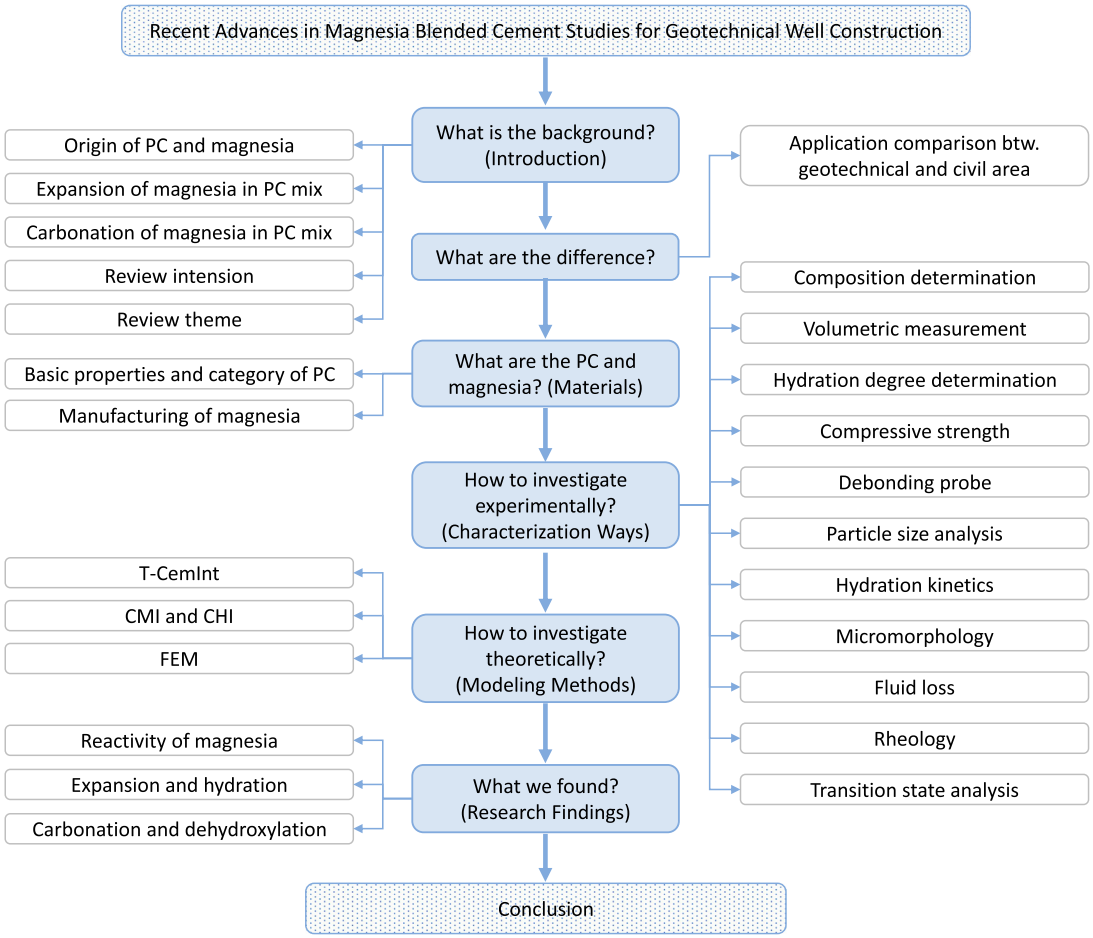

FIGURE 1 | Review structure diagram.

Meanwhile, the hydration product of magnesia, brucite has been studied as the high potential carbon dioxide fixation candidate (Jung et al., 2004; Aminu et al., 2017). Magnesia blended Portland cement also has the capability of neutralizing CO_2 footprint (Zhang et al., 2018). Owing to its lower energy requirement and carbon footprint, the reactive magnesia blended Portland cement has become one of the principal global CO_2 mitigation practices in the construction material domain (Unluer and Al-Tabbaa, 2013).

Extensive studies have been included which were conducted on magnesia blended Portland cement, not only in the civil construction domain, but also in the geotechnical well construction area. The authors believe that a structured review paper that presents the recent technical evolvement on magnesia blended cement will be meaningful and important to understand the potential of using magnesia as part of the Portland cement replacement to alternate cement sheath properties in terms of underground applications. Hence, the valuable technical legacies will probably further promote the corresponding research in the geotechnical well constructions such as making use of certain positive properties of magnesia (expandable, thermally stable, carbonation capability) to mitigate geotechnical well cementing issues (debonding, micro-annulus, calcium leaching because of carbonation).

The current study presents a literature review on the studies of incorporation of magnesia (magnesium oxide) into Portland cement material from the geotechnical well construction perspective. Starting with the comparison of the application conditions between conventional civil construction and geotechnical well cementing, this work reviewed the Portland cement categorizations, magnesia manufacturing routes at first. Then, the experimental characterization methods have also been elucidated including composition determination, particle size analysis, volumetric variation measurement, compressive strength testing, shear-bond strength testing, etc. Meanwhile, the development of cement material hydration modeling methods is also summarized which potentially facilitates the analysis of magnesia hydration and expansion on the mechanical properties of Portland cement mix. The physical-chemical-mechanical properties of magnesia and blended Portland cement are investigated which includes the reactivity of magnesia, expansion influence from its hydration, and carbonation/dehydroxylation of magnesia blended Portland cement. Moreover, the results and conclusions were extracted from the literature. The detailed review structure diagram is shown in **Figure 1**. Through this route, a comprehensive

TABLE 1 | Cement material application conditions comparison.

	Civil construction	Geotechnical well construction
Geometry and volume	Diverse geometry structures. Enormous volumetric occupation is sometimes required such as hydro-dam, foundation, and main frame of building constructions	Almost similar geometry structure—circular cylinder shell form with very high length/radius ratio and length/thickness ratio and limited volume
Curing pressure	Atmospheric pressure	Normal hydrostatic pressure commonly increased with well depth Abnormal hydrostatic pressure resulted from geological structural impact, thermal-fluid effectetc.,
Curing temperature	Natural atmospheric temperature between –50°C and 90°C	Petroleum engineering: 0°C–200°C Geothermal energy: commonly 100°C–300°C CCS (CO_2 capture and sequestration): similar to petroleum engineering
Surrounding fluid	Air; Fresh water; Sea water	Formation water with different salinity and constituents Acidic formation fluid (CO_2 enriched, H_2S enriched) Hydrocarbon fluid/natural gas
Mechanical loadings	Static mechanical loadings dynamic mechanical loadings e.g. earthquake (occasionally)	Dynamic loadings arising from the drilling operation, production operation, and sequestration operation
Technical standard	Based on ASTM C150 ASTM International, (2019a), categorized into 5 types (Type I to Type V) and 5 sub-types (Type IA, Type IIA, Type II-MH, Type II-MH-A, Type IIIA)	Based on API 10A American Petroleum Institute, (2019)(referenced with ASTM C465 ASTM International, (2019b), C150 ASTM International, (2019a), C114 ASTM International, (2009), etc.), categorized into 8 types (Class A to Class H). Most commonly used - Class G has more stringent manufacturing requirements than others

understanding of the scientific research progress on magnesia blended Portland cement development for geotechnical well construction is derived.

2 APPLICATION CONDITIONS: GEOTECHNICAL WELL CEMENTING VS CIVIL CONSTRUCTION

As for the most dominant cement, PC was applied in oil wells for the first time in 1903 (Piot, 2020). This happened after 79 years of PC being patented. As mentioned above, the application conditions for cement materials are very distinct between civil construction and geotechnical well construction. These distinctions can be found in the following **Table 1**.

Because of such differences, especially the much more harsh service conditions and the difficulties of their recurrence in lab scale, it is worth endeavoring to probe and characterize the properties of cement materials and bridge potential technical measures to address or mitigate industrial application problems.

3 MATERIALS - PORTLAND CEMENT AND MAGNESIA

3.1 PC Categorizations and Basic Properties

Since the PC came into the scientific study domain and engineering application for almost two centuries, many researchers conducted quite an amount of theoretical, numerical, and experimental studies on this topic. Some consensus of PC components has been accepted broadly by the present scientific and engineering circles. The main constitutions in PC regardless of its type, e.g. 10 types as per ASTM (American Society for Testing and Materials) (ASTM International, 2019a) or 8 types as per API (American Petroleum Institue) (American Petroleum Institute, 2002) standards actually, are alite (tri-calcium silicate or $3CaO{\cdot}SiO_2$ or C_3S), belite (di-calcium silicate or $\boldsymbol{\beta}$ – $2CaO{\cdot}SiO_2$ or C_2S), celite (tri-calcium aluminate or $3CaO{\cdot}Al_2O_3$ or C_3A), felite or ferrite (Frederick and Thomas, 2020; Gutteridg and Pomeroy, 1983) (tetra-calcium alumino-ferrite or $4CaO{\cdot}Al_2O_3{\cdot}Fe_2O_3$ or C_4AF), and gypsum (calcium sulfate dihydrate or $CaO{\cdot}SO_3{\cdot}2H_2O$ or $C\bar{S}H_2$). The first four phase-notations were invented by Le Chatelier (Chatelier and Mack, 1905) and Törnebohm (Blezard, 1998; Poole and Sims, 2016). Some other minor components possibly exist which come from the different clinker precursors such as the dead burnt magnesia, the sulfates residual, the alkalis (commonly sodium oxide and potassium oxide), etc. These constituents of PC can be elaborated in oxides concentration or cementitious phases concentration that is listed in **Table 2**. As (Michaux et al., 1989) said, PC hydration speed relies on the relative concentrations of the cementitious components and their particle size or fineness. API (American Petroleum Institute, 2002), ASTM (ASTM International, 2019a), and some researchers (Ramachandran and Feldman, 1996) use some qualitative and quantitative compositions of these cementitious phases to categorize the PC. The summary of these categorizations can be found from one table including five sub-tables (**Supplementary Tables S1–S5**) in the Supplementary Material.

Because PC is the dominant binder material in construction engineering, there are detailed restrictions on the oxides and

TABLE 2 | PC oxides composition.

PC oxides composition				
Oxide	**Composition (wt%)**			
—	Soroka, (1979)	Lawrence, (1998)	Neville and Neville, (2011)	Barnes and Bensted, (2002)
CaO	60–67	58.1–68	60–67	60–70
SiO_2	17–25	18.4–24.5	17–25	18–22
Al_2O_3	3–8	3.1–7.56	3–8	4–6
Fe_2O_3	0.5–6	0.16–5.78	0.5–6	2–4
MgO	0.1–5.5	0.02–7.1	0.5–4.0	sum < 5%
$Na_2O + K_2O$	0.5–1.3	0.04–2.64	0.3–1.2	—
TiO_2	0.1–0.4	—	—	—
P_2O_5	0.1–0.2	—	—	—
SO_3	1–3	0–5.35	2.0–3.5	—

mineralogical compositions, e.g. the lime content must meet some specific requirements. The too high content of lime (> 67%) will probably leave free lime after setting which will cause unsoundness issues (Soroka, 1979). On the contrary, a too low content of lime will slow down the hydration and setting process of the Portland cement apparently (Soroka, 1979) which makes it difficult to meet the civil and geotechnical well construction needs.

Apart from the lime content, another two main oxides in PC, alumina (Al_2O_3) and ferrous oxide (Fe_2O_3), also play a vital role in its physicochemical properties. Firstly, alumina (usually in the form of C_3A) and ferrous oxide (usually in the form of C_4AF) govern the setting time of PC. Gypsum ($C\bar{S}\cdot 2H$) addition, the function of which is to control the setting time of PC, only works under a certain threshold of SiO_2/R_2O_3 ratio as 1.5 (Soroka, 1979). The notation of R_2O_3 refers to the total amount of alumina and ferrous oxide. Secondly, less composition of C_3A means less susceptibility to sulfate attack. So, the sulfate-resistant grade of different PC is generally classified based on C_3A content.

Commonly, higher content of C_3S compared with C_2S and finer particle size indicates quicker hydration rate and development of initial mechanical strength. By tuning the concentration of C_3S, C_2S, C_3A, and the particle size, different fit-for-purpose PC will be made to qualify diverse engineering requirements.

3.2 Magnesia Manufacturing

3.2.1 Source Materials

As the constitution of 2% of Earth's crust and the third abundant element in seawater, magnesium has been exploited by human beings for over two centuries. In Earth's crust, magnesium-containing minerals cover a wide range such as chlorites, pyroxene, and amphibole group minerals, dolomite, magnesium-calcite, magnesite, hydrated carbonates, brucite, and salt deposits. In respect of exploiting natural minerals, sedimentary layers play a vital role in human history where the main constituents of magnesium minerals are the dolomite group and phyllosilicates group (e.g. chlorite, glauconite). Dolomite group accounts for around 30% of the carbonates in sedimentary layers which are approximately equivalent to 4.6×10^{15} tonnes of magnesium. However, the geological distribution of magnesium-bearing minerals is very erratic. Since the divalent bonding property and comparable cation size with respect of magnesium, calcium, and iron, the isomorphism always exists in the dolomite-brunnerite-ankerite group minerals where the relative phase composition fluctuates among magnesite ($MgCO_3$), calcite ($CaCO_3$), and siderite ($FeCO_3$) (Shand, 2006c).

3.2.2 Manufacturing Routes

There are commonly two methods to obtain magnesia products: mining and calcining magnesium-bearing minerals (magnesite, brucite, or dolomite); synthesis magnesium compound from seawater and subsequent calcination. The first one prevails the latter because of much higher energy consumption and more complicated processes regarding the latter path. To get magnesia (MgO), calcination of magnesite and brucite [$Mg(OH)_2$] is the most popular measure.

$$MgCO_3 \xrightarrow{550^\circ C - 750^\circ C} MgO + CO_2\uparrow \quad (1)$$

$$Mg(OH)_2 \xrightarrow{>350^\circ C} MgO + H_2O\uparrow \quad (2)$$

From **Equation (1)** and **(2)**, these thermal decomposition equilibriums rest on two factors: temperature and partial pressure of gas phases (e.g. CO_2 or H_2O). Any of these two parameters changes (temperature going up or gas partial pressure decreasing) will cause the decomposition reaction proceeding (Liu et al., 2017). The impurities content and crystal structure of magnesite minerals will affect this decomposition temperature range (Shand, 2006c). If the source material of calcination is dolomite, the calcite composition in this solid solution[1] will affect the thermal decomposition very much. Based on the work of (Mitchell, 1923), the calcination firstly caused the decomposition of dolomite into calcite and magnesite:

$$CaCO_3 \cdot MgCO_3 \xrightarrow{\simeq 500^\circ C} CaCO_3 + MgCO_3 \quad (3)$$

The dissociation of CO_2 from magnesite will proceed afterward as per **Eq. (1)**. It should be noted that the calcite

[1]This is not yet conclusive based on some research results. Mitchell etc. stated that with our present knowledge it is impossible to decide definitely whether the dolomite is a singular point in a series of solid solutions, or whether it is a compound. (Mitchell, 1923).

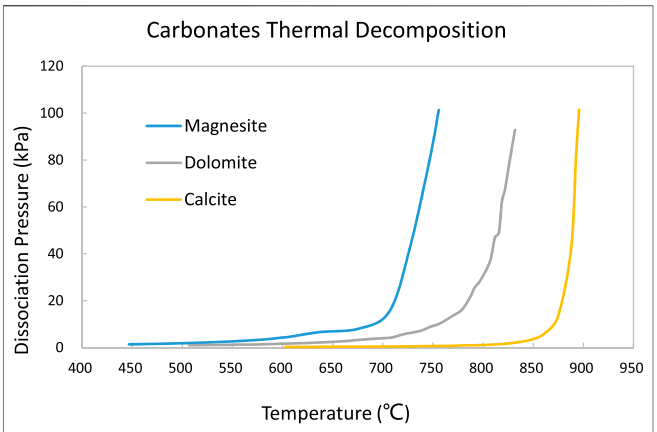

FIGURE 2 | Carbonates thermal decomposition. After (Mitchell, 1923).

content in dolomite will also take dissociating process when temperature increased to a certain level [875°C–900°C under 1 atm/101.3 kPa CO_2 partial pressure **Figure 2**, (Mitchell, 1923), or 812°C–950°C under 26.7 kPa of CO_2 partial pressure (Hashimoto et al., 1980)]. Hence, to control the magnesia quality, the calcination temperature should be manipulated within the proper range if the source material is dolomite.

3.2.3 Calcination of Source Materials

3.2.3.1 Magnesite/Dolomite

To illustrate the micro calcination decomposition process, the "shrinking shell" model (Shand, 2006a) was proposed which seems like a "peeling" process from outside inward on crushed magnesite/dolomite ore pieces. The real calcination progress inside the rotary kiln can be divided into several stages sequentially from pre-heat, calcination, residence, sintering, to cooling stage as the result of burners arrangement and their firing scenarios. Ore feed size, the temperature profile of calcination, the crystalline structure of ore minerals and even ore feed shape have significant impacts on the thermal decomposition of magnesite ores and the quality of magnesia. Optimized manufacturing must balance such factors as production rate, product (magnesia) quality, energy consumption/cost. In general, the following relations always co-exist:

- Higher calcination temperature means faster dissociating of CO_2 from ore, a higher extent of crystallization of magnesia, and lower reactivity.
- Calcination curing time plays a similar role as temperature.
- Finer ore feed size and more uniform shape also benefit from faster expelling of CO_2 and more uniform "peeling" of ore pieces, however no doubt, the energy requirement and cost of the pre-handling of ores increases.

The standard heat of thermal dissociation of magnesite to magnesia and carbon dioxide is 3,027 kJ/kg (723 kcal/kg) after Knibbs's work (Knibbs and Benn, 1924). Based on Shand's work (Shand, 2006a), the decomposition energy requirement of magnesite is 2,415 kJ/kg (577 kcal/kg) which includes the pre-heating energy from ambient temperature (25°C) to decomposition temperature (750°C) and thermal decomposition itself (enthalpy of magnesite decomposition at 1,000 K is 1,284 kJ/kg).

3.2.3.2 Brucite

Magnesium hydroxide, or $Mg(OH)_2$, also named brucite in some cases, is another source material for making magnesia products. Nevertheless, this production route can be further categorized into two directions: calcining synthesized brucite filter cake through the "wet method", or direct calcination on brucite ore through the "dry method" on account of its origin.

Once two models were postulated to describe the calcination decomposition mechanism of brucite around the 1960s (Goodman and Bowden, 1958; Ball and Taylor, 1961; Brindley and Hayami, 1963). No conclusion has been drawn in this respect yet. Nonetheless, the consensus tends to be that the decomposition of brucite comprises the processes of nucleation and crystal growth of magnesium oxide inside the brucite matrix and the diffusion of water molecules from it. During this decomposition, the cryptocrystalline size of precursors (either synthesized magnesium hydroxide or natural brucite) impacts the micro-crystalline formation. Whether or not the intercrystalline fissures resulting from exceeding the contraction stress happen depends on the cryptocrystalline size of precursors. If the nascent $Mg(OH)_2$ crystal size is less than 60nm, few fissures will appear during its decomposition. The crystal size of commercial $Mg(OH)_2$ products are both exceeding this value: 1 μm–15 μm for natural brucite, 0.5 μm–2.5 μm for synthetic $Mg(OH)_2$ (Rothon and Hornsby, 2014). Therefore, when the calcination proceeds, the micro-fissures of magnesium hydroxide will cause sudden crystal conversion from the hexagonal/rhombohedral unit as $Mg(OH)_2$ to the cubic unit as MgO. Simultaneously, the H_2O is formed from adjacent layers of hydroxyl groups combination (Shand, 2006a).

The energy demand using the "wet method" is higher than the "dry method" since the remarkable existence of balanced water (28–50% by weight (Shand, 2006a),) in synthesized brucite sludge. Plus the relatively high specific heat capacity of water (4,200 kJ/kg), the manufacturing of magnesia from synthesized brucite is energy-intensive. The standard heat requirements (calcining brucite from ambient temperature as 25°C to the critical decomposition temperature as 350°C) of obtaining magnesia by thermal dissociating CO_2 from brucite are 6,347 kJ/kg through the "wet method" and 1,498 kJ/kg through the "dry method" respectively. The fundamental decomposition abides by the process as **Eq. (2)**. The chemical-bonded water is hard to be fully liberated from brucite under the medium thermal effect except the temperature reaches over 1,000°C (Gregg et al., 1955).

4 EXPERIMENTAL CHARACTERIZATION METHODS

Because of the composite material characteristics of Portland cement and its multi-dimensional properties (physical, chemical, mechanical), a number of characterization experimental methods

can be applied to investigate a certain property with regards to surrounding conditions. Based on this review work, the main characterization methods have been summarized for future reference.

4.1 Composition Determination

4.1.1 X-ray Diffraction

X-ray diffraction (XRD) is a typical non-destructive technique used in materials science. It can determine the chemical composition and crystallographic structure of a material by irradiating it with incident X-rays and measuring the intensities and scattering angles of the leaving X-rays from the targetted material (Sima et al., 2016). Most of the technical research works relevant to cement materials will use this powerful method to verify the composition of source materials and hydrated/carbonated products. As for the magnesia blended Portland cement, this method can give us the qualitative and quantitative [with Rietveld method and Bogue method (Samudio, 2017)] description of magnesia, hardened cement specimen, brucite, magnesite, and hydrated magnesium carbonates, etc.,.

4.1.2 X-ray Fluorescence

X-ray fluorescence (XRF) is a well-established technique for materials analysis. By illuminating the analyzed sample with X-rays, the core-level electrons in the sample will be excited to a higher energy level. Then the decay radiation from these excited electrons back to their original ground level results in the emissions of "secondary" X-rays or fluorescent. This radiation represents the characteristic of the energy levels of every atomic species and thereby can be used as a spectroscopic fingerprint for these elements (Simon, 2018). Almost all the chemical oxides composition data from the referenced literature in this work are derived by use of this method.

4.1.3 FTIR

FTIR, denoting Fourier Transform Infrared Spectroscopy, is a reliable and established method to analyze the mineralogical compositions of rocks (Srivastava et al., 2018). This technique was gradually developed through three milestones which are infrared light (discovery by Frederick William Herschel in 1800 (Khan et al., 2018)), Michelson interferometer (invented by Albert Abraham Michelson in 1880 (Smith, 2011)), and Cooley-Tukey Algorithm/FFT [made by J. W. Cooley and J. W. Tukey in 1966 (Johnston, 1990; Smith, 2011)] respectively. Because of its advantages such as Fellgett advantage (fast analysis speed), Jacquinot advantage with high sensitivity, simple mechanical structure with low requirements of maintenance, self-calibration capability, repeatability, it has become the horsepower technology in the material characterization analysis field for over 70 years (ThermoScientific, 2020). Thanks to modern computer algorithms development, aside from qualitative analysis, FTIR can also be used as a reliable quantitative analysis measure (Hänchen et al., 2008; Ballirano et al., 2010; Dung and Unluer, 2016, 2017; Zhang et al., 2017; Srivastava et al., 2018).

4.2 Shrinkage/Expansion Measurement

4.2.1 Direct Measurement of Chemical Shrinkage and Bulk Shrinkage

Chemical shrinkage can be measured by monitoring the absorbed water volume when the corresponding cement samples are water-bathed. This method is not an accurate one, even the water exchange control with the outside environment is guaranteed because the water access capability from the inside pore system of cement samples will gradually decrease coupled with the hydration process going. In other words, the realistic complete hydration cannot be achieved (Baumgarte and Thiercelin, 1999). Similarly, bulk shrinkage can also be measured directly regarding the cement sample's bulk volume change after designated curings with three methods. The first one is called the "membrane test" method with the sealed condition (API, 2015). The second measure is using the annular ring test which is included in the API recommended practice (API, 2015). This standard, also as a part of ISO 10426 ISO (2004), recommends basic practices on determining "stiff-enough" cement matrix expansion during the hydration period under atmospheric pressure conditions. Some modified protocols based on this instruction emerged for a while that aimed to apply varied hydraulic pressure and temperature conditions. Many valuable experimental investigations and results have been obtained by use of this method which evolves our understanding of cement matrix volume variation in the process of hydration, especially on the oil well cement systems. However, similar to the linear measurement method, it has limited capabilities which cannot reflect the downhole surroundings' impacts regarding high temperature, high pressure, and various water source supply situations Onaisi et al. (2019). Aside from these cons, monitoring cement matrix volume shrinkage coupled with hydration evolution in real-time is impossible by use of such a method. The third way is to survey the linear autogenous strain (Sant et al., 2006; Lura and Jensen, 2007) under the assumption of isotropic deformation. Linear autogenous strain can be monitored with watertight corrugated molds equipped with a dilatometer (Jafariesfad et al., 2017b). This measurement method is only able to monitor the linear strain under low temperature (below water boiling temperature) and atmospheric pressure conditions.

4.2.2 Embedded Strain Gauge

For linear shrinkage/expansion measurement, one simple method is to use needle-like indicators embedded in the ends of cured samples and dial caliper to measure the expansion extent periodically in the curing process of samples (Ogawa and Roy, 1981). The pros of this method is that the measuring process is comparatively easy to do. The disadvantages are the discontinuous surveys when the samples curing, the inconvenient demolding of curing samples from a mold after the initial set process (several hours to days depending on the experiment plan; to make sure the sample ends' integrity and the survey needle indicators consistent position embedded into the ends of samples before curing commence), the limited survey

accuracy because of the measuring tool's capability [this will be more evident when dealing with the samples with delicate volume change at the beginning time of solidification by using a caliper whose accuracy is just around 0.01 mm or even less (Britannica, 2019)], and the limited curing conditions (usually the curing conditions for this measurement is within the low temperature (less than 90°C) and low pressure (atmospheric pressure) domains).

4.2.3 Cement Hydration Analyzer

Cement hydration analyzer (CHA) is a real-time cement paste volumetric variation method developed in recent years. By injecting gas (e.g. N_2) from the bottom of the slurry sample and monitoring the flow rate of this gas entering the cement with gas mass flow meter, the shrinkage/expansion of the cement specimen can be measured with respect to the volume change of the pressurized water that is contacting the specimen. Some experimental and analyzing instrumentation vendors like Chandler have this kind of product with relatively high-temperature (163°C) and high-pressure grades (6.9 MPa).

4.2.4 Slurry-to-Cement Analyzer

In recent years, thanks to the development of experimental instrumentation, some comprehensive investigation devices such as Slurry-to-cement analyzer (STCA), have turned up that can examine the volumetric change of cement during the hydration process coupled with simulating *in-situ* downhole conditions (Vu, 2012; Agofack, 2015; Samudio, 2017; Onaisi et al., 2017, 2019). As per the publication literature, it seems that the original set-up idea is inspired by the tri-axial rock mechanics experimental instruments. This facility can test cement specimens under varying or fixed stress and temperature conditions by monitoring specimens' strain and pore pressure variation in real-time. Both strain and internal pore pressure variation relate to the micro and bulk volume change of cement samples. Moreover, this facility has other functions aside from thermal and pore pressure tests like isotropic stress tests and deviatoric stress tests. So more thorough and realistic understandings of the shrinkage/expansion behavior of cement can be achieved in the light of this method. One interesting matter that needs to be pointed out is that some valuable conclusions made by these works are based on the cement internal pore pressure survey capability while this has not been clearly illustrated in these pieces of literature. Some other literature shows their advancements in measuring cement internal pore pressure (Zhang et al., 2019). The main novelty of their work is the experimental setup for pore pressure monitoring. This setup can control surrounding pressure around the cement specimen by use of the water bath method. Using an embedded pressure gauge to monitor the cement pore pressure variation during the hydration process is the key survey measure which was sealed with a flexible but impermeable membrane to prevent cement slurry invasion to the sensor. Valuable comparisons with other similar studies have been done in this work. Generally speaking, the experimental results matched other results. A parallel conclusion can be drawn based on these comparisons. However, because of the set-up design, it also has some shortcomings: 1) without thermal control; 2) limited pressure grade (1,500 psi pressure was used in the study). In a word, although the functions of this method (Zhang et al., 2019) are different from the previous one's (Onaisi et al., 2017, 2019), the basic idea of this research output still has its values.

4.3 Determination of Hydration Degree

4.3.1 X-Ray Diffraction

The XRD-based analysis is capable of verifying the hydration degree of a certain composition in set cement. Since XRD analysis is based on crystalline structure features of materials, this method is preferable to the crystal stuff. Since the common inorganic expandable hydration products (like magnesium hydroxide) in the PC-based mixture are in the crystalline state, the qualitative confirmation of magnesia and magnesium hydroxide existence and the quantitative analysis of hydration degree of magnesia can be obtained with this method Vandeperre et al. (2008); Aphane (2007).

4.3.2 Differential Scanning Calorimetry (DSC)

Differential scanning calorimetry (DSC) is also an option to quantitatively analyze the hydration degree of certain cementitious materials. This method is based on the assumption that different crystal structures of materials will cause different dehydration endothermal activity. We can use the standard reference calorimetry curve to match each sample's dehydration endothermal behavior and to obtain each characteristic material's composition/concentration in the mixture. Pre-requisites of DSC analysis:

- Finely ground sample.
- Good heating control.
- Reference material as the endothermal standard. Usually a metal like pure tin takes this role which will melt at 232°C at the cost of 14.2 cal heat transformation.

4.3.3 Calorimeter

Calorimeter testing can also be used to determine the hydration degree of cement paste/slurry. This method is based on the exothermic feature of cement hydration. The total released heat during cement hydration can be estimated by means of the constituents of the cement specimen and corresponding methods from such studies Vu (2012); Lura et al. (2003). Since the calorimeter can measure the cumulative heat released from cement slurry's hydration in real-time, the hydration degree can be evaluated with the following equation (LibreTexts, 2019):

$$DoH\,(t) = \frac{Q(t)}{Q_{Total}} \tag{4}$$

where: $Q(t)$ is the released heat (kJ) during cement slurry hydration at time t, Q_{Total} is the total released heat (kJ) when the cement slurry specimen is completely hydrated, $DoH\,(t)$ is the degree of hydration (%).

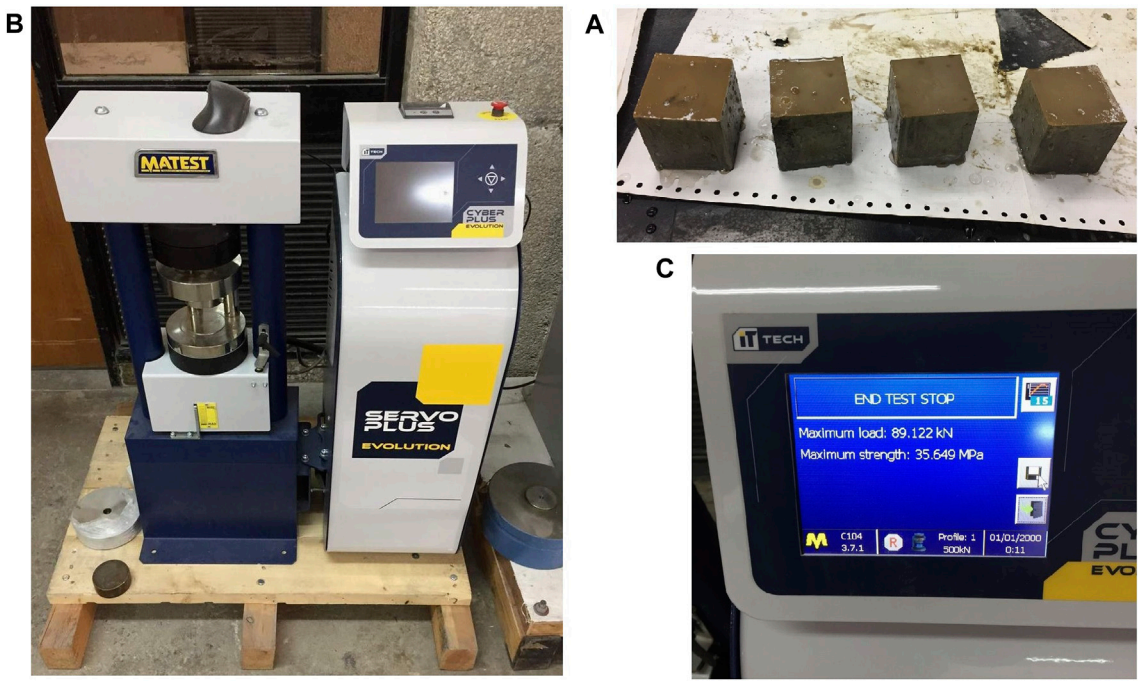

FIGURE 3 | Cement specimens, uniaxial loading equipment, and UCS test result sample. **(A)** is a batch of demolded cured cement specimens. **(B)** is a set of uniaxial loading equipment to do the crushing test. **(C)** is a screen shot of one UCS test result sample.

4.3.4 Ultrasonic Cement Analyzer Deduction

Besides the above three ways, some researchers (Onaisi et al., 2017) used the Ultrasonic Cement Analyzer (UCA) to deduce the hydration degree of cement slurry hydration. Usually, UCA has been standardized as the non-destructive compressive strength measurement method (ref. **Section 4.4.2**). Since UCA can "monitor" the evolution of compressive strength of cement system, while the compressive strength development has a certain correlation with the hydration process, some deduction method is obtained through the following equation:

$$DoH\,(t) = \frac{V_p\,(t) - V_{p-int}}{V_{p-\infty} - V_{p-int}} \tag{5}$$

where: V_p (t) is the monitored compression wave velocity (in/microsec) during cement slurry hydration at time t, V_{p-int} is the initial compression wave velocity (in/microsec) during cement slurry hydration, $V_{p-\infty}$ is the final compression wave velocity (in/microsec) when the cement slurry specimen is completely hardened, DoH (t) is the degree of hydration (%).

4.4 Compressive Strength Determination

4.4.1 Destructive Crushing Method

Destructive compressive strength measurement on cement samples has been standardized in ASTM and API (ASTM International, 2020; API, 2013). After curing at designated temperature and pressure conditions for a certain period (e. g. 24 h) within specified cubic molds with 2-in dimensions, cement specimens (**Figure 3**) will be demolded and crushed by the uniaxially loading frame (**Figure 3**) with pre-required loading rate [72 ± 7 kN per minute if expected compressive strength > 3.5 MPa; 18 ± 2 kN per minute if expected compressive strength ≤3.5 MPa (API, 2013)]. The compressive strength (**Figure 3**) obtained by this method is named the unconfined uniaxial compressive strength (UCS). Before the emergence of UCA, this is the principal investigation way to quantify one of the key mechanical properties of cement samples. Furthermore, based on the correlation analysis between UCS results and ultrasonic longitudinal wave velocity monitoring, this technique paved the way for developing UCA (Rao et al., 1982; Thiercelin, 2006).

4.4.2 Non-destructive Measurement Method

In the present non-destructive compressive strength practices, UCA (Ultrasonic Cement Analyzer, **Figure 4**) dominates this application since it is the only procedure that can monitor the evolution of some mechanical properties (elastic modulus, compressive strength) in real-time (**Figure 4**) without intervening in the hydration process. Because of this overwhelming advantage, this technique gains its privilege in cement lab investigation (Backe et al., 2001). Meanwhile, this method has been incorporated into the API standard (API, 2013). The original idea was invented by (Rao et al., 1982). Through decades of development and application, a huge amount of lab experimental research works has been benefitted from this technique (Backe et al., 2001; Vu, 2012; Agofack, 2015; Samudio, 2017; Agofack et al., 2019).

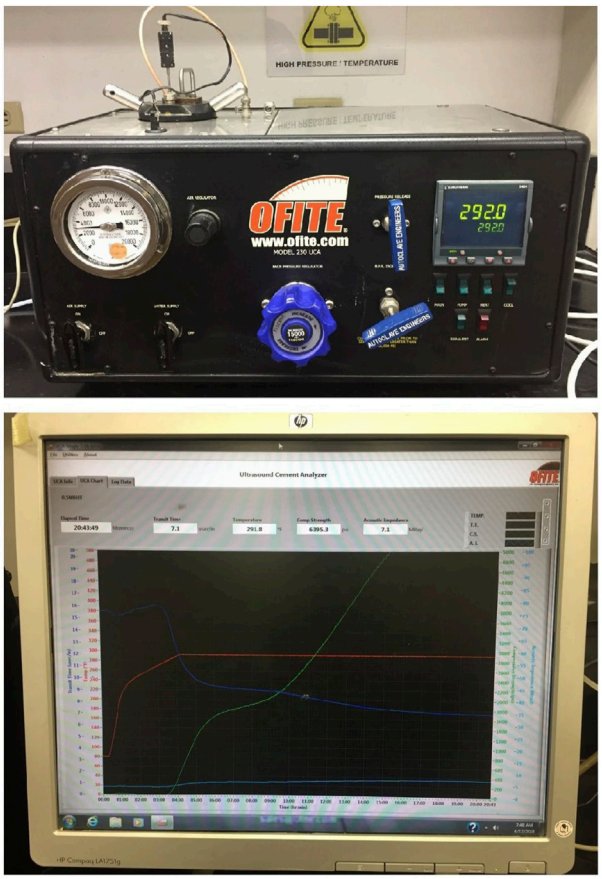

FIGURE 4 | UCA Device and Monitoring Curve Sample. **(A)** is a UCA device. **(B)** is one UCA monitoring curve sample).

4.5 Debonding Probe

The debonding phenomenon refers to the physical separation at the cementing interfaces (casing and cement sheath, cement sheath and formation). This is also called "micro-annulus" in the geotechnical well construction field. Avoidance and addressing the debonding issue is the first order of maintaining well integrity. In the petroleum engineering industry, investigation of debonding existence, extent, and location has become the core of cementing quality assessment. CBL and VDL are the commercialized technologies capable of accomplishing this job. Based on the logging mechanism of CBL, some researchers invented a lab-scale acoustic measurement unit (see **Figure 5**) which had been used to evaluate the closing micro-annulus capability of magnesia blended PC (Thomas J. et al., 2014).

As **Figure 6** shown below, the impedance maps for the expansive cement specimens (W/C = 41%, 6% BWOC of dead burnt magnesia, 6% BWOC of dead burnt lime) were conducted at 115 h (just before the heat treatment—cured at 30°C) and at 139 h (just after the heat treatment - curing temperature increased from 30°C to 66°C). Before the heat treatment, the acoustic impedance map on the left, shows zero impedance everywhere with red color, indicating a dry micro-annulus at the first cementing interface. Nonetheless, after the heat treatment, the acoustic impedance map on the right shows good cementing bonding all around the casing demonstrating that the heat-activated expansion from magnesia was able to close a pre-existing micro-annulus and restore the acoustic coupling between the cement and inner casing.

4.6 Particle Size Determination Methods

Particle size has an important role in the cement hydration process. For instance, even for the same materials, they will hydrate at different rates which affect the thermal equilibrium of hydration, the acidic/alkaline environment, and produces diverse hydration products. The

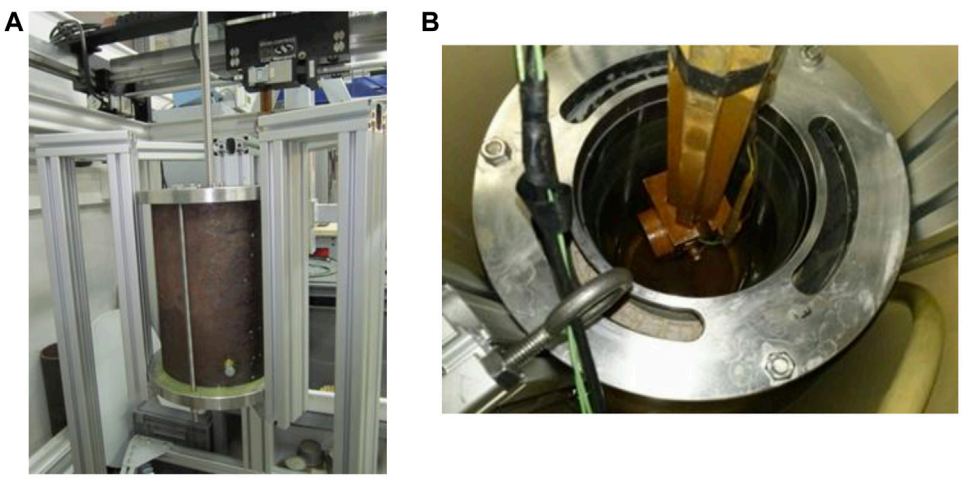

FIGURE 5 | Lab scale simulated cemented annulus unit and acoustic logging apparatus. **(A)** is the side view. **(B)** is the side view. After (Thomas J. et al., 2014).

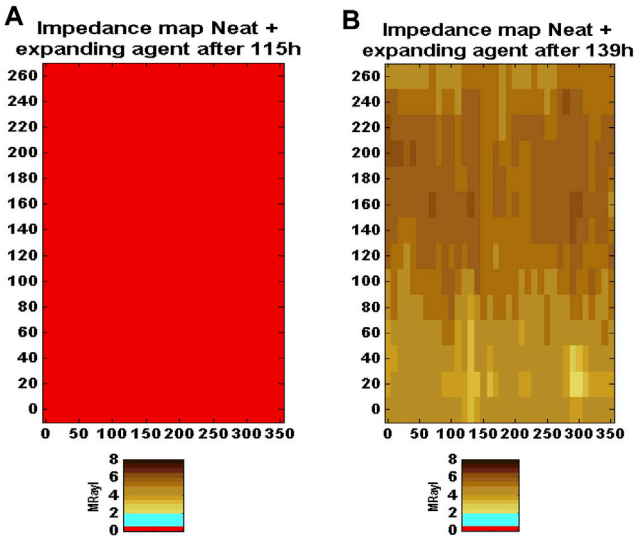

FIGURE 6 | Acoustic impedance maps for the expansive cement formulation after reducing the casing pressure. **(A)** is the impedance map before the heat treatment (after 115 h curing at 30°C). The impedance values are close to zero everywhere, indicating the presence of a complete dry microannulus. **(B)** is the impedance map after 8 h heat treatment at 66°C and 8 h normal curing at 30°C (after 115 h curing at 30°C). Acoustic coupling has been restored, indicating that the microannulus has closed. After (Thomas J. et al., 2014).

measurement methods of particle size or particle size analysis have been also developed for over one century corresponding with the development of material science. For cement and cement-based material research, several methods can be used such as the sieve method (Aphane, 2007; Liska et al., 2008; Liska and Al-Tabbaa, 2009, 2012; Mo et al., 2010; Panesar and Mo, 2013; Dung and Unluer, 2016; Ruan and Unluer, 2017; Mo and Al-Tabbaa, 2020), dynamic light scattering (Jafariesfad et al., 2017b), laser scattering (Shand and Jin, 2020), SEM (Qafoku et al., 2015), Blaine specific surface area method (Al-Tabbaa, 2013).

4.7 Hydration Kinetics Monitoring

As described in **Section 4.3.3**, the calorimetry is a useful measure to monitor the exothermal heat accumulation during cementitious material hydration. Hence, this technique is the usual way to analyze the hydration kinetics projecting the cement slurry formulations variations and their potential interacting impacts. For example, in (Thomas J. et al., 2014) research, the authors found out that the retardation effect probably behaved mono-directionally from PC to magnesia.

4.8 Micromorphology

Scanning electron microscopy (SEM) is one of the principal characterization methods for imaging the micromorphology and microstructure of materials. By projecting a beam of low energy electrons onto the material sample, some detector will be used to monitor the photons and electrons emitted from the interaction between the source beam electrons and the sample atom electrons. If equipped with other energy-dispersive X-ray microanalysis functions (such as EDX, EDS), this technique can determine the composition and orientation of individual crystals or features (Omidi et al., 2017; Raval et al., 2019). Similar to XRD and XRF, almost all the research work cited in this work used this method to investigate the micromorphology and microstructure characteristics of target materials and to provide the scientific evidence corresponding to certain analysis.

4.9 Transition State Analysis

As mentioned in **Section 2**, the application conditions of cement material in a geotechnical well construction field is much different from that in the civil construction area. When pumping the prepared cement slurry into the downhole annulus, the transition state development in the setting and hardening process has to meet several engineering demands such as having a long enough pumpable time to place the slurry as desired, quick gel strength evolvement to facilitate the prevention of formation gas/liquid intrusion as much as possible, and fast mechanical strength advancement to resume afterward operation as soon as possible. Therefore, to verify these properties and figure out the transition state regimes in the lab are significant to the successful cementing job. This is also applied to the magnesia blended Portland cement system. So, three aspects corresponding to the aforementioned properties will be illustrated as follows as thickening time, transition time, and wait-on-cement (WOC) time respectively.

4.9.1 Thickening Time

The thickening time test is an exclusive lab test method fit for the geotechnical well cement slurry. Thickening time is used to indicate for how long a time the cement slurry could be in a pumpable state when exposed to geotechnical well downhole conditions (temperature, pressure). It is important for the cementing operation at the wellsite. Hence, it must be assessed in the lab by simulating the pumping temperature regime and replacement downhole conditions with a pressurized consistometer (Ghofrani and Plack, 1993; Shakirah, 2008; Srivastava et al., 2018) under dynamic conditions (stirred at 150 ±15 rpm) before field trials/applications. A plot of "viscosity" (consistency in Bearden units or shorted as Bc) of the tested slurry versus time will be depicted. With the proper settings of the thickening time experiment, the elapsed duration when the tested Bc value reaches 70 Bc is commonly defined as the thickening time. The details of the apparatus requirements, testing procedure, and determination of test schedules can be found in (API, 2013).

4.9.2 Transition Time

Transition time is used to describe the static gel strength development of cement slurry. It reflects the slurry changes from the complete hydraulic fluid to a highly viscous gel showing some semi-solid characteristics under static-state conditions (Rogers et al., 2005). This is one of the necessary properties of the cement slurry to prevent the possible formation gas/fluid intrusion into the setting cement matrix (Rogers et al., 2004). Although this testing method is not standardized, the main cement property testing instrument vendors have developed the corresponding devices to measure the static gel strength evolvement like MACS II of FANN, Model 5,265 of

CHANDLER, and 120–58 of OFITE. The basic measuring mechanism is similar to the pressurized consistometer (measuring the thickening time) except the stirring rate would be very slow (e.g. 0.26°/min or 1 round/23 hrs). The typical transition time is defined as the elapsed duration when the static gel strength of tested slurry evolved from 100 lbf/100 ft^2 to 500 lbf/100 ft^2 (or 4,788 Pa to 23,940 Pa) (Rogers et al., 2005).

4.9.3 Wait-On-Cement Time

Wait-on-cement time is the duration of cement slurry developing to a certain compressive strength after the slurry was placed into the annulus properly. It also describes how fast the cement slurry could develop into a solid state. This term contributes to the cost control of drilling operation due to how soon afterward the drilling operation could be resumed. Since this indicator relates to the compressive strength, the ultrasonic cement analyzer (UCA) can be used to quantify it. Usually, the duration of compressive strength evolving from 100 psi to 500 psi is defined as the WOC (Rogers et al., 2005; Backe et al., 2001; Ridha et al., 2013). For the test procedure, refer to **Section 8** of (API, 2013).

4.10 Fluid Loss

The fluid loss reflects the relative effectiveness of a cement slurry to retain its water phase when exposed to a differential pressure condition with a filter medium (e.g. geological formation). Too much fluid loss/filtrate means the cement slurry undergoing dehydration which will cause a series of quality issues of cement sheath (micro-annuli, bonding issue, etc.,). Some researchers pointed out that the incorporation of magnesia particles into Portland cement will increase the slurry's fluid loss quantity (Brandl et al., 2014). Other studies also used such a testing method to evaluate the possible impact of magnesia introduction into Portland cement (Ghofrani and Plack, 1993; Hammad and Altameini, 2002). The testing procedures and requirements can also be found in (API, 2013). As for the static fluid loss test, the prepared slurry will be poured into a specially designed cell with the 325 mesh screen mounted at the bottom. After applying a 1,000 psi differential pressure and opening the bottom valve, the accumulated fluid volume filtered out within 30 min will be measured and doubled as the fluid loss if without the gas blow through.

4.11 Rheology

Rheology properties of cement slurry directly influence the efficiency of slurry placement and displacement rate of drilling fluid (Shahriar and Nehdi, 2012; Tao et al., 2019). In the field, it also impacts the pumpability and mixability of the cement slurry. The specific experimental procedure has been included in (API, 2013). Three parameters (plastic viscosity, yield point strength, and gel strength) are employed to describe several fundamental properties of cement slurry during the pumping process. Plastic viscosity affects the flow regime of cement slurry. The turbulent flow regime and viscous property of flowing cement slurry are both beneficial to enhance the displacement rate of drilling fluid. Hence, the proper plastic viscosity gained means the compromised result between these two factors which is desired under certain operation conditions (Murtaza et al., 2019). Yield point strength always correlates with the anti-setting capability of cement slurry. Higher yield point strength indicates that the cement slurry shows a lower tendency to settle down its solid particles with relatively better vertical homogeneity. The gel strength reflects how easy to activate/resume the flowing state of cement slurry after keeping it static for a while. Relative lower gel strength facilitates the commence of the pumping process and lowers the requirements of cementing pump devices. Some researchers have pointed out the values or studies these rheological properties regarding magnesia blended oil well cement (Ghofrani and Plack, 1993; Hammad and Altameini, 2002; Srivastava et al., 2018; Jafariesfad et al., 2020).

5 MODELING STUDIES

Compared with the advancement of experimental studies, the modeling studies on the correlation between the hydration of cementitious materials and their corresponding mechanical properties are limited. Due to the expansion mechanism of magnesia hydration on the Portland cement system, the output of three related modeling studies has been outlined below. These methods can analyze the correlation between the hydration of cementitious materials and their corresponding mechanical properties by considering different factors such as volumetric properties and stress conditions. Therefore, using these methods will potentially facilitate the analysis of the impact of magnesia hydration and expansion on the mechanical properties of the Portland cement mix.

5.1 T-CemInt Modeling

In recent years, an applicable modeling program has been developed which can be used to analyze the stress evolution and pre-stress situations during the cement paste hydration under different simulated downhole surrounding conditions (Onaisi et al., 2017, 2019). The core equations of their modeling methods are listed below.

$$\begin{cases} \delta\sigma_{r_f} = 2\left(\lambda_f + G_f\right)A_f - 2G_f\dfrac{B_f}{r^2} - \dfrac{\alpha_f E_f}{1-\nu_f}C \\ \delta\sigma_{\theta_f} = 2\left(\lambda_f + G_f\right)A_f + 2G_f\dfrac{B_f}{r^2} + \dfrac{\alpha_f E_f}{1-\nu_f}(C-\delta T) \\ \delta\sigma_{z_f} = 2\lambda_f A_f - \dfrac{\alpha_f E_f}{1-\nu_f}\delta T \end{cases} \tag{6}$$

$$\begin{cases} \delta\sigma_{r_{cas}} = 2(\lambda_{cas} + G_{cas})A_{cas} - 2G_{cas}\dfrac{B_{cas}}{r^2} - \dfrac{\alpha_{cas}E_{cas}}{1-\nu_{cas}}C \\ \delta\sigma_{\theta_{cas}} = 2(\lambda_{cas} + G_{cas})A_{cas} + 2G_{cas}\dfrac{B_{cas}}{r^2} + \dfrac{\alpha_{cas}E_{cas}}{1-\nu_{cas}}(C-\delta T) \\ \delta\sigma_{z_{cas}} = 2\lambda_{cas}A_{cas} - \dfrac{\alpha_{cas}E_{cas}}{1-\nu_{cas}}\delta T \end{cases} \tag{7}$$

$$\begin{cases} \delta\sigma_{r_c} = 2(\lambda_c + G_c)A_c - 2G_c\dfrac{B_c}{r^2} - 3K_{bc}\delta\varepsilon_{exp} - b_c\delta P_{pore} - \dfrac{\alpha_c E_c}{1-\nu_c}C \\ \delta\sigma_{\theta_c} = 2(\lambda_c + G_c)A_c + 2G_c\dfrac{B_c}{r^2} - 3K_{bc}\delta\varepsilon_{exp} - b_c\delta P_{pore} + \dfrac{\alpha_c E_c}{1-\nu_c}(C-\delta T) \\ \delta\sigma_{z_c} = 2\lambda_c A_c - 3K_{bc}\delta\varepsilon_{exp} - b_c\delta P_{pore} - \dfrac{\alpha_c E_c}{1-\nu_c}\delta T \end{cases} \tag{8}$$

$$C = \frac{1}{r^2}\int_{r_i}^{r}\rho\delta T\partial\rho \tag{9}$$

$$\begin{cases} \dfrac{\partial T}{\partial t} = D_{cas}\left[\dfrac{\partial^2 T}{\partial r^2} + \dfrac{1}{r}\dfrac{\partial T}{\partial r}\right] \\ \dfrac{\partial T}{\partial t} = D_f\left[\dfrac{\partial^2 T}{\partial r^2} + \dfrac{1}{r}\dfrac{\partial T}{\partial r}\right] \\ \dfrac{\partial T}{\partial t} = D_c\left[\dfrac{\partial^2 T}{\partial r^2} + \dfrac{1}{r}\dfrac{\partial T}{\partial r}\right] \end{cases} \tag{10}$$

$$\begin{cases} 2(\lambda_{\text{cas}} + G_{\text{cas}})A_{\text{cas}} - \dfrac{2G_{\text{cas}}}{r_{\text{icas}}^2}B_{\text{cas}} = -\delta P_{pore} \\ 2(\lambda_{cas} + G_{cas})A_{cas} - \dfrac{2G_{cas}}{r_{ocas}^2}B_{cas} - 2(\lambda_c + G_c + M_c b_c^2)A_c + \dfrac{2G_c}{r_{ocas}^2}B_c \\ \qquad = \dfrac{\alpha_{cas}E_{cas}}{1-\nu_{cas}}C_{cas} - 3K_{bc}\left(1 + \dfrac{M_c b_c}{K_{sc}}\right)\delta\varepsilon_{\text{exp}} + M_c b_c(\gamma_c\delta\xi_c - 3\alpha_{mc}\delta T) \\ r_{ocas}A_{cas} + \dfrac{B_{cas}}{r_{ocas}} - r_{ocas}A_c - \dfrac{B_c}{r_{ocas}} = -\dfrac{1+\nu_{cas}}{1-\nu_{cas}}\alpha_{cas}r_{ocas}C_{cas} \\ 2(\lambda_c + G_c + M_c b_c^2)A_c - \dfrac{2G_c}{r_{hole}^2}B_c - 2(\lambda_r + G_r)A_f + \dfrac{2G_r}{r_{hole}^2}B_f \\ \qquad = (1 - 2M_c b_c^2)\dfrac{\alpha_c E_c}{1-\nu_c}C_c + 3K_{bc}\left(1 + \dfrac{M_c b_c}{K_{sc}}\right)\delta\varepsilon_{\text{exp}} - M_c b_c(\gamma_c\delta\xi_c - 3\alpha_{mc}\delta T) \\ r_{hole}A_c + \dfrac{1}{r_{hole}}B_c - r_{hole}A_f - \dfrac{1}{r_{hole}}B_f = -\dfrac{1+\nu_c}{1-\nu_c}\alpha_c r_{hole}C_c \\ r_{ob}A_f + \dfrac{1}{r_{ob}}B_f = -\dfrac{1+\nu_c}{1-\nu_c}\alpha_c r_{ob}C_f \end{cases} \tag{11}$$

where, subscripts of *f*, *c*, *cas*, *ob*, *hole*, *ocas*, *icas* refer to the surrounding formation, cement paste/slurry, casing, the outer boundary of formation, the outer diameter of casing, the inner diameter of casing respectively; subscripts *r*, *θ*, and *z* denote radius direction, circumferential direction, and borehole axial direction respectively; σ means stress; λ and G are Lame coefficients; r is the radius from wellbore center; α refers to the linear thermal expansion coefficient; E denotes the elastic modulus; ν is the Poisson's ratio; ρ means density; T denotes temperature; K_b is the bulk incompressibility modulus; ε_{exp} denotes the expansion strain; b denotes Biot coefficient; P_{pore} is the pore pressure inside of cement specimen; γ is the pore pressure-hydration coupling parameter; ξ_c is the cement hydration degree; **Eqs. 6–8** are the stress-strain equilibrium equations of casing, cement paste/sheath, and formation; **Eq. (10)** are the temperature profile in casing, cement, and formation; **Eq. (11)** can be used to calculate the intermediate parameters of *A* and *B*.

Based on the assumptions from their work (Onaisi et al., 2017, 2019) and by applying some laboratory measurements and homogenization techniques, all the specific directional-based stresses and strains components can be obtained. Radial tensile crack development and debonding scenarios can be analyzed by using the Mohr-Coulomb criterion Onaisi et al. (2017).

Given the directional stresses, strains, and other parameters shown in **Eqs (6)–(11)**, the main equations governing the coupling effect regarding cement paste/sheath between pressure, stress, strains (shrinkage or expansion) can be acquired with such equations:

$$\begin{cases} \delta\sigma_{mean} = K_{b_c}\delta\varepsilon_{vs} - 3K_{b_c}\delta\varepsilon_{l_{exp}} - b_c\delta P_{pore} \\ \dfrac{\delta P}{M_c} = -b_c\delta\varepsilon_{mean} - 3(1-b_c)\delta\varepsilon_{exp} - \gamma_c\delta\xi_c + \dfrac{\delta m_w}{\rho_w} \\ \gamma_c = \dfrac{\rho_w + \rho_{cas}\text{R}_{wc\_H}}{\rho_w + \rho_{cas}\text{W/C}}\varepsilon_{ish} \\ \delta\phi = \left[\gamma_c - \phi_0\dfrac{\text{R}_{wc\_H}}{\text{W/C}}\right]\delta\xi_c \end{cases} \tag{12}$$

where subscripts of *c* and *w* refer to cement and water respectively; R_{wc_H} is the mass ratio of water to cement grains consumed by hydration reaction; W/C denotes the water to cement ratio by mass; ε_{ish} means the cement internal shrinkage; ϕ refers to the porosity in cement paste/sheath; ϕ_0 refers to the initial porosity in cement paste/sheath.

5.2 CMI and CHI Modeling

T-CemInt model is a hydration modeling method that mainly focuses on the mechanical and relevant volumetric properties of cement paste hydration. The cement sheath integrity is not only about mechanical characteristics, but also including hydraulic features. Bois et al. proposed a crossing check method on a cement plug by use of cement mechanical integrity (CMI) and cement hydraulic integrity (CHI) models (Bois et al., 2019). Although they didn't give the complete set of equations, the hypotheses, physical case configurations, and specific parameters have been illustrated in their paper. The novelty of their work is the introduction of the porous media idea into the existed hydration modeling and taking into account the surrounding formation fluids exposure scenarios.

Formulated on the hypotheses and configurations (Bois et al., 2019), coupling analysis was conducted between the fluid pressure variation (hydraulics) and the solid-matrix stiffness (mechanics) at the micro-annulus area with introducing CHI simulation techniques. Some insightful conclusions were acquired as:

- The most probable integrity risk comes from the micro-annulus formed at the second cementing interface (interface between cement plug and wellbore formation). Other failure risks such as compression or tension exist but at much lower possibilities.
- Enhancing the mechanical properties like compressive strength, tensile strength will not benefit the hydraulic integrity of cement plug.
- Desaturation and less access to water of the cement paste during hydration will facilitate the creation of micro-annulus in the form of the capillary effect.
- After the formation of micro-annulus at the second cementing interface, the hydraulic pressure decay will rely on hole diameter, sealing efficiency of a plug, plug depth, and some of the rheological properties (viscosity, compressibility) of wellbore fluid above the plug. Micro-annulus propagation (aperture) will behave contrary to the both stiffness of the formation surrounded and the

cement plug itself. Hydrophobic wellbore fluid will make more micro-annulus development than the hydrophilic one because of the former's limited penetration capability into set cement and corresponding limited mitigation of capillary pressure decrease after hydration.

- The inclusion of post-hydration expansive admixtures/additives probably improves the hydraulic integrity status of the set plug while further investigations on this topic need to be done afterward.

5.3 FEM Modeling—The Impact of Pre-stress Resulting From the Expansion on the Mechanical Integrity of the Cement Sheath

In order to investigate the influence of pre-stress status caused by the expansion (e. g. mineral brucite formation) on the cement matrix mechanical integrity, Patel et al. used the Finite Element Modeling (FEM) method and acquired some perceptive findings (Patel et al., 2019). Their work included two parts: 1) the effect of different pre-stress conditions on the mechanical integrity of set cement; 2) sensitivity analysis between them. Their physical model included three parts as the inner liner, the intermediate cement sheath, and the outer casing unit. The loading condition only covered the wellbore pressure imposed on the inner liner. The cementing interface between liner and cement sheath was the study interest. For the sake of conducting the FEM simulations, they validated their FEM model by comparison with the analytical calculation (based on the thick-walled concentric cylinder model) results of radial and hoop stress under different wellbore pressure conditions. They found that the compressive pre-stress is dominated by and proportional to the linear expansion while it impacted the cement sheath mechanical integrity only marginally. The expansion would benefit mitigating the radial cracking probability by compensating the hoop stress with compressive pre-stress status. However, some further studies need to be conducted on the shear stress failure risk in terms of the expansion-induced pre-stress.

6 HYDRATION, CARBONATION MECHANISMS, AND CHARACTERISTICS RELATED TO PC AND MAGNESIA

Generally speaking, the physical and chemical properties of magnesium oxide (MgO, magnesia) are heavily dependent on several factors viz. precursor type and its morphology, calcination temperature and residence time, impurities types, and content. The priorities of these factors also can be deemed as such sequence (Shand, 2006f).

As for the physical properties, there are lots of recorded data based on previous literature such as crystal structure, density, specific surface area (SSA), luster, color, hardness, index of refraction, thermal conductivity, specific heat capacity, electrical resistance, thermal expansion, melting point, boiling point, standard enthalpy of formation, standard Gibbs free energy of formation, etc., **Supplementary Table S6** in the Supplementary Material lists some of them in respect of the underground applications.

As for the chemical attributes, in light of underground circumstances, the reactivity, dissolution, hydration, carbonation will be summarized here.

6.1 Reactivity of Magnesia

First of all, the reactivity of MgO matters in the hydration process of magnesia blended Portland cement. Talking about this means it hardly bypasses the SSA. The positive correlation between them is evident (Shand and Jin, 2020; José et al., 2020). Higher SSA means higher reactivity of MgO particles (Jin and Al-Tabbaa, 2020). This also illustrates the importance of calcination conditions during the manufacturing of MgO. The impact of calcination temperature and residence time have similar impacts to the calcination of magnesia precursors, not only magnesite or dolomite but also brucite. Usually, beyond the critical decomposition temperature, 350°C for brucite, 500°C for dolomite or magnesite, lower temperature with shorter residence time (15–25 min) will produce a higher specific surface area of MgO (ref **Figure 7**). Hence, the calcination temperature of producing caustic magnesia commonly is between 400°C and 1,000°C (Unluer and Al-Tabbaa, 2013). For example, 52 years ago (Smithson and Bakhshi, 1969), already pointed out that the calcination temperature and residence time dominate the particle size and crystalline content of produced MgO from precursors. When calcined below 500°C, MgO particle size can be less than 10 nm; above 1,000°C, MgO particle size can reach more than 100 nm. This range varies among different pieces of literature, probably because of the different contents of impurities of precursor materials.

Another factor is the crystal structural features. On account of the coordination number of the Mg atom/ion, it is impossible to fabricate the perfect crystal structure of MgO even it is the simplest form of crystalline-like halite. In more detail, the surface defects can be depicted from plane view and 3D view. In the two-dimensional view, the surface of MgO is always born with defects such as steps, kinks, vacancies, adatoms, and fissures (Sushko et al., 2002). In the three-dimensional view, the existence of apexes/corners/edges of cryptocrystalline plus the coordination unsaturation of Mg atom/ion magnifies the defect severities. These defects become the front of hydration because they provide the vulnerable zone for ion exchange and corresponding water molecule chemisorption (Shand, 2006f).

The pH value of solution media plays a vital role in the dissolution and hydration of MgO (Shand, 2006f; Fruhwirth et al., 1985). Some pH-dependent rate-controlling processes can be summarized as follows (at room temperature):

$$MgO + H_2O \xrightarrow{pH>7} Mg^{2+} + 2OH^- \quad (13)$$

$$MgO + 2H^+ \xrightarrow{pH<5} Mg^{2+} + H_2O \quad (14)$$

The process of **Eq. (14)** is the proton attack at the crystal structure of MgO and hereafter the desorption of cation Mg^{2+} and hydroxyl anion, especially at the defect spots. However, the

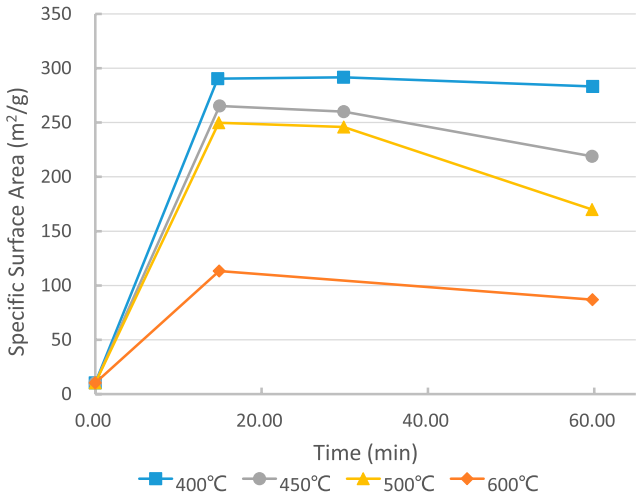

FIGURE 7 | Thermal decomposition vs SSA of magnesia (precipitated magnesium hydroxide). After (Shand, 2006a).

process regarding **Eq. (13)** is the adsorption of hydroxyl anion at the defect spots and desorption of cation Mg^{2+} and hydroxyl anion from the crystal surface. Pure proton diffusion probably happens in the case of the pH as between 5 and 7.

Besides the impacts of reactivity of MgO and pH surroundings on the dissolution and hydration of MgO, the exposure of MgO with H_2O molecule simultaneously occurs as the chemisorption of H_2O. This adsorption is part of dissolution and afterward hydration. How easily the chemisorption emerging relies also on the characteristics of the defects of the cryptocrystalline of MgO as mentioned above. In a word, less crystal defect means the lower tendency of water molecule chemisorption (Onishi et al., 1987; Peng and Barteau, 1990).

The hydration process can be regarded as several steps: water molecule reaction with MgO surface layer to produce $Mg(OH)_2$, dissolution of such $Mg(OH)_2$, and exposure of fresh solid MgO particle surface for hydration proceeding. Nevertheless, the solubility of $Mg(OH)_2$ is very limited which makes the removal of $Mg(OH)_2$ "coating" very slow (Smithson and Bakhshi, 1969; Fruhwirth et al., 1985; Khangaonkar et al., 1990). On the other hand, the reactivity of magnesia depends strongly on its particle size and crystal defects. Lower calcination temperature with shorter residence time makes the calcined magnesia with smaller particle size and more crystal defects. Therefore, these characteristics facilitate the magnesia hydration progressing more readily.

6.2 Expansion and Hydrated Matrix Structure Alternation

When we discuss the expansion behavior and properties of magnesia blended cement, it is inevitable to mention its rival—shrinkage. What the shrinkage issue deteriorates and what this may cause are mostly the aspects that the expansion behavior needs to cope with.

Shrinkage issue is an intrinsic feature and issue accompanied by hydration of cement material. At present, this issue can be categorized into several types: chemical shrinkage, self-desiccation (autogenous shrinkage), and thermal shrinkage.

- Chemical shrinkage arises from the fundamental property of cement hydration which means the hydration products occupy less volume than the reactants (Sant et al., 2006; Scrivener et al., 2016). Some estimated chemical shrinkage value may be around 6.25 ml/100 g BWOC (by weight of cement) (Baumgarte and Thiercelin, 1999).
- Autogenous shrinkage is also defined as self-desiccation induced bulk shrinkage which roots from the capillary force and an under-pressure in set cement matrix pore solution that is transferred to the bulk solid matrix to cause it to contract (Bentur et al., 2001; Lura et al., 2003; Chen et al., 2013). Some researchers also defined the bulk shrinkage as the external cement sample dimensions change (Baumgarte and Thiercelin, 1999; Reddy et al., 2009). The bulk shrinkage varies in the range of 0.5–5% (Parcevaux and Sault, 1984; Justnes et al., 1994, 1995) and highly correlates with the curing conditions.
- Thermal shrinkage usually refers to the late age bulk shrinkage during the mass cement/concrete structure cooling period which is caused by the volume thermal expansion during the initial setting period and the poor thermal conductivity of mass cement/concrete structures (Mo and Panesar, 2012; Mo et al., 2014).

Why is addressing the shrinkage issue important? It will benefit the well integrity more or less which mainly arises from cement sheath mechanical properties like bonding strength at cementing interfaces, internal tensile strength, stress condition, elastic properties, etc.,.

First of all, shrinkage will increase the probability of debonding incidents at both of the cementing interfaces. Micro-annulus is probably caused by certain shrinkage issues which could induce formation fluid migration and sustained casing pressure (SCP) (Reddy et al., 2009). Besides the SCP phenomenon, the micro-annulus issues can usually be validated with the loss or weak response of CBL (cement bond log) and VDL (variable density log) logging at wellsite (Baumgarte and Thiercelin, 1999; Gowida et al., 2018). Although formation fluid migration (especially gas migration) has been categorized into three types (Stiles, 2006) which all demanded bundle of cement slurry/sheath properties (Ravi et al., 2002; David; Stiles, 2006; Williams et al., 2011; Shadravan et al., 2014; Jafariesfad et al., 2017a), the volume stability is always on the list.

Secondly, shrinkage is always coupled with cement pore pressure decrease during the hydration process. With the hydration going on, the original cementitious clinker materials will react with water to produce certain products, mostly as C-S-H gel/phase. This hydration will cause a chemical shrinkage phenomenon which results in the porous matrix and capillary effect during cement setting. The solution media in the pores contributes to the pore pressure. This plays a critical role in the initial internal stress condition of the set cement sheath which further connects internal cracking issues (Onaisi et al., 2017; Zhang et al., 2019). Pore pressure variation indicates two meaningful factors for shrinkage mitigation/expansion activation:

- Water supply. If the cement sheath was under drained conditions, it would get the water supply from the surroundings. This scenario refers to the downhole cementing contacting with water-bearing formation. Since some of the expansive additives activate their expansion through their hydration reactions, the water supply (between internal pore structure and formations) matters in two senses: how much the expansive additive is hydrated and how much pore solution residue there is. Lack of water supply with on-going hydration and condense matrix formed in the pores will make the pore pressure drop below the surrounding pressure.
- Pore pressure channeling. With water supply condition means with a fluid flow channel between the pore structure of the cement both inside and surrounding the formation. These micro-channels can not only provide the water supply but also provide the pressure transmission tunnels with the internal pore structure of cement. This channeling will decrease the effective stress inside the cement matrix (semi-hardened state during hydration). If the effective stress decreased below the expansion stress (resulted from "crystal growth" (Baumgarte and Thiercelin, 1999; Yang et al., 2019; Guren et al., 2021), the bulk expansion effect will be activated then.

Expansive cement, as one of the effective measures mitigating or addressing the shrinkage and self-cracking issues, has become the study topic for over one century. In this work, the term expansive cement refers to the PC mixed with the expansive agents. The aim of using this material is to counter the shrinkage effect and realize the controlled volume expansion to maintain its volume consistency in the construction area and the primary sealing capability in the downhole annular space. Self-healing cement is a synonym of expansive cement under some circumstances (Zhang et al., 2020). Enhanced autogenous healing can be facilitated through non-encapsulated additions such as magnesia. Aside from this, if micro-cracks/internal cracks formed after the cement set, the microencapsulated healing technique can be the remedial candidate. The core materials include mineral expansive additives like magnesia (Mao et al., 2020).

On the crystal growth based pathways, magnesia mixed cement has also been successfully applied in the geological well fields because of its higher tolerance to high temperature (Ghofrani and Plack, 1993; Nelson and Drecq, 1990; Appah and Reichetseder, 2002), lower water consumption (Nagataki and Gomi, 1998), controllable hydration (Mo et al., 2010; Jafariesfad et al., 2016), lower hydration enthalpy (Ghofrani and Plack, 1993), and lower carbon dioxide leaching tendency (**Section 6.3**). Moreover, the blending of reactive MgO with PC does not interact with each other to produce the new hydration products except their hydration products (brucite and C-S-H gel), respectively (Vandeperre et al., 2008). However, regarding hydration kinetics, the blending of magnesia with PC behaves differently from each other (Thomas J. et al., 2014). Magnesia hydration will be substantially retarded while the PC hydration will behave as usual. One possible reason can be attributed to the pore solution chemical conditions such as pH value variation, different ionic components (silicate ions, aluminate ions). Some other researchers, (Brandl et al., 2014), gave another version of magnesia's impact on PC hydration. They commented on two side-effects of magnesia on PC hydration: 1) acceleration of PC hydration and setting; 2) increment of fluid loss of cement slurry.

Along with shrinkage mitigation, soundness is another important factor that needs to be considered. ASTM standards requires that the maximum expansion extent should be 0.8% (ASTM International, 2019a). However, some studies have shown that under certain magnesia dosages (<5%), there is no evident observation of unsoundness phenomena (Moradpour et al., 2013).

Mitigating shrinkage issue is not only significant to the volume stability of set cement matrix itself but is also vital to some other key properties such as flexibility. As (Jafariesfad et al., 2017a) mentioned, increasing the flexibility of the set cement matrix is to improve the ratio of tensile strength versus Young's modulus or as σ_t/E. Fibers (micro-fiber, nano-fiber) and nano-particles are usually incorporated into the cement formulation regarding this aim. Besides this, coupled with high resistance to reciprocated loading regimes during well production processes and low shrinkage properties is preferred. For instance, shale gas development always requires volumetric fracturing after well completion which demands the cement sheath with good bonding properties and flexibility. Some researchers (Williams et al., 2011) pointed out that some quantitative expansion ratios

such as between 0.2% and 0.5% should be met to reduce the SCP (sustained casing pressure) as much as possible.

As we know, the hydration of cement paste/slurry always proceeds with the induction period at the beginning time. From the study results of (Ogawa and Roy, 1982), the bulk volume variation also undertook the process from the chemical shrinkage (the extent rested on the formulation of cement slurry) to the gradual expansion. Besides this, the expansion rate and hydration degree of the sample also behaved higher when the curing temperature was higher. Meanwhile, these two values also reached a plateau earlier than the lower curing temperature samples. Apart from the reactivity of magnesia affecting its hydration rate, the aging conditions such as curing temperature also impact its hydration rate. Therefore, the question of how to realize the optimum expansion from magnesia hydration corresponding with the hydration progress of Portland cement already aroused some researchers' interests. In 1993, Reza Ghofrani et al. pointed out this issue in their study of the expansion effect from dead-burnt magnesia (calcined at 1,400°C) and lime (calcined at 1,400°C) on neat Portland cement slurry under atmospheric and HPHT (high-pressure, high-temperature) conditions (Ghofrani and Plack, 1993). The choice of these two oxide expansive additives should depend on the downhole temperature. The calcium oxide (calcined at 1,400°C) is fit for the temperature of less than 70°C. And the magnesium oxide (calcined at 1,400°C) is fit for the case of higher temperature up to 175°C. In addition, the shear bond strength (at the cementing interfaces) was improved by the bulk expansion, and the permeability of the hardened cement sample was decreased on account of the *in-situ* expansion in the pore matrix of set cement. Jafariesfad et al. (Jafariesfad et al., 2017b) investigated the impact of magnesia with different reactivity (70–260 nm in average particle size) on the expansion and tensile strength of some oil well cement slurry. They employed near ambient aging conditions (40°C, atmospheric pressure) to cure their cement specimens. Based on their results, it is promising to obtain the acceptable tuning between shrinkage compensation and sustained mechanical strength of cement sheath by manipulating the reactivity of magnesia.

6.3 Carbonation of Magnesium Hydroxide, Dehydroxylation of Magnesium Carbonates

The carbonation of magnesia or magnesium hydroxide originally arose from the purification of MgO (Doerner et al., 1946; Sheila et al., 1991; Shand, 2006e). During the carbonation process, the chemisorption of CO_2 with the MgO crystal surface probably happens as reaction **Eq. 15**. The lattice oxygen in MgO crystal is essentially prone to attract acidic molecules such as CO_2 to produce surface CO_3^{2-} (Ochs et al., 1998).

$$CO_{2\,(\text{interface})} + O^{2-}_{(\text{interface})} \rightarrow CO^{2-}_{3\,(\text{interface})} \tag{15}$$

At the same time, because of the co-existence of H_2O, MgO, and CO_2, the following reactions/processes also will take place under atmospheric pressure (CO_2 partial pressure) and ambient temperature conditions (20°C) (Fernández et al., 1999):

$$CO_2\,(\text{gas}) + H_2O_{(\text{liquid})} \rightarrow CO_{2\,(\text{aqueous})} \tag{16}$$

$$CO_{2\,(\text{aqueous})} \leftrightarrow CO_{2\,(\text{interface})} \tag{17}$$

$$MgO_{(\text{solid})} + H_2O_{(\text{liquid})} \rightarrow Mg(OH)_{2\,(\text{solid})} \tag{18}$$

$$CO_{2\,(\text{interface})} + Mg(OH)_{2\,(\text{solid})} + (n-1)H_2O_{(\text{liquid})} \rightarrow MgCO_3 \cdot nH_2O_{(\text{solid})} \tag{19}$$

$$MgCO_3 \cdot nH_2O_{(\text{solid})} + CO_{2\,(\text{interface})} \leftrightarrow Mg^{2+}_{(\text{interface})} + 2HCO^{-}_{3\,(\text{interface})} + (n-1)H_2O_{(\text{liquid})} \tag{20}$$

$$Mg^{2+}_{(\text{interface})} + 2HCO^{-}_{3\,(\text{interface})} \leftrightarrow Mg^{2+}_{(\text{aqueous})} + 2HCO^{-}_{3\,(\text{aqueous})} \tag{21}$$

Processes 16 to 21 will occur when there is enough dissolved CO_2 in the solution. Through these reactions, more carbon will be trapped in magnesium bicarbonate compounds. However, if the dissolved CO_2 decreased or the temperature of the solution increased, the magnesium bicarbonate compounds would precipitate magnesium carbonate compounds (e.g. hydromagnesite) and produce CO_2 from the solution. One example can be illustrated as the following reaction **Eq. 22**:

$$5Mg(HCO_3)_{2\,(\text{aqueous})} \rightarrow Mg_5(CO_3)_4(OH)_2 \cdot 4H_2O_{(\text{solid})}\downarrow + 6CO_{2\,(\text{gas})}\uparrow \tag{22}$$

This decarbonization process will proceed as the dehydroxylation reactions with regards to solubility decreased trend (ref. to **Supplementary Table S5** in the Supplementary Material) as follows (Langmuir, 1965; Davies and Bubela, 1973) **Eq. 23**:

$$\underset{\text{Lansfordite}}{MgCO_3 \cdot 5H_2O} \overset{10^{\circ}C}{\rightarrow} \underset{\text{Nesquehonite}}{MgCO_3 \cdot 3H_2O} \overset{55^{\circ}C}{\rightarrow} \underset{\text{Hydromagnesite}}{Mg_5(CO_3)_4(OH)_2 \cdot 4H_2O} \tag{23}$$

Even though the above carbonation mechanisms were obtained from the leaching magnesia pulp, the fundamental reactions are also applicable to the magnesia/brucite carbonation in terms of the carbon dioxide capture and sequestration (also abbreviated as CCS). Extensive studies have been conducted on this hot topic especially in the latest decades because of the greenhouse effect issue (Zhang et al., 2017). Among these works, some of them focused on the carbonation of civil binder materials including brucite, magnesia cement (no PC content), and magnesia blended cement (with PC content) under ambient conditions (normal temperature, ambient CO_2 partial pressure). Others targeted the carbonation of magnesium silicate mineral and magnesia blended cement with respect to high-temperature, high-pressure (CO_2 partial pressure) conditions. Meaningful findings extracted from these works will shed light on the CO_2 geological sequestration and relevant geotechnical well constructions.

Some studies targeted the carbonation of neat brucite (between CO_2 gas and brucite solid) (Béarat et al., 2002). The dehydroxylation, carbonation, and rehydroxylation mechanisms were investigated under different CO_2 partial pressure, different temperatures, and different morphological factors. Several

insights of the dehydroxylation/carbonation of brucite are as follows:

- Carbon dioxide (CO_2) pressure and temperature have vital roles in the carbonation process of brucite.
- Corresponding to a certain temperature, the CO_2 has a threshold value which makes the carbonation proceed. Beyond this threshold, increasing CO_2 pressure probably causes the passivation of the carbonate layer which will slow down the proceeding of carbonation reactions.
- Destruction of the passivation layer is the key to continuous carbonation inward. Translamellar cracking, delamination, and morphological reconstruction attribute to this destruction (based on lamellar brucite structure).
- Below the thermodynamically unstable temperature of magnesite ($MgCO_3$) and at a constant carbon dioxide (CO_2) pressure, increasing temperature will increase the carbonation reactivity.

More investigations have been carried out on the enhanced carbonation of reactive magnesia blended cement materials under ambient temperature/pressure and different CO_2 concentrations. The experimental details summary can be found from one table including five sub-tables (**Supplementary Tables S7–S11**) of the Supplementary Material. Since portlandite would be formed after Portland cement hydration, some researchers studied the carbonation mechanism when portlandite and brucite co-exist in suspension (Silva et al., 2009). Inclusion of magnesium carbonate phase into calcium carbonate system can improve the strength property by means of introducing magnesium hydroxide into calcium hydroxide slurry exposed to CO_2 carbonation curing. The Mg/Ca ratio of the initial mix determines the strength performance variation. The CO_2 pressure and curing duration impact the strength property differently based on the initial Mg/Ca ratio. The magnesium-bearing carbonate contents [$(Ca,Mg)CO_3$ and $MgCO_3{\cdot}3H_2O$] are favored with higher CO_2 pressure and longer carbonation curing duration.

Based on the results from (Hopkinson et al., 2008), when suspending magnesia into some solution ($CaCl_2$) at a mol ratio of 5:1, the transition phase (transitory magnesium hydrate carbonate, $MgCO_3{\cdot}2H_2O$) can be formed in the transformation process from nesquehonite to hydromagnesite and depends strongly on the curing period, the porous aqueous solution chemical composition, and the *in-situ* crossings of supersaturation limits. Meanwhile, the geochemical response, from dissolution to precipitation process between calcite and transitory hydromagnesite phases, can accelerate the transition from nesquehonite to hydromagnesite.

Dung and Unluer found the positive effects of hydration agent (HA) and dispersant agent (DA) on accelerated carbonation of reactive magnesia suspension (Dung and Unluer, 2016): the HA (e.g. HCl) can improve the conversion from magnesia to brucite in both rate and amount aspects; the DA [e.g. $(NaPO_3)_6$] can delay the precipitation of brucite and facilitate its direct carbonation in pore solution. These two agents facilitate the afterward HMCs [hydrated magnesium carbonates, nesquehonite—$MgCO_3{\cdot}3H_2O$, hydromagnesite—$4MgCO_3{\cdot}Mg(OH)_2{\cdot}4H_2O$, dypingite—$4MgCO_3{\cdot}Mg(OH)_2{\cdot}5H_2O$] formation and the micromorphology variation (denser matrix, larger HCMs crystal size), which in turn benefits the compressive strength gain in the short term (28 days), e.g., 115% and 58% higher than the control mix with ambient carbonation and accelerated carbonation respectively.

In terms of ternary magnesia cement (reactive magnesia, PFA—pulverized fly ash, natural aggregates like sand and gravel) (Unluer and Al-Tabbaa, 2014), the carbonation and afterward mechanical performance development is dependent on such factors as water/cement ratio (w/c ratio), CO_2 concentration, curing duration, RH (relative humidity), and wet/dry cycling frequency. They are influenced by each other. PFA addition is beneficial to the carbonation rate and extent of this system. Shorter carbonation duration prefers lower w/c ratio mix and vice versa. CO_2 concentration has an optimal value in terms of maximum carbonation extent because the higher CO_2 concentration of 20% is reflected by the similar mechanical property compared with the lower CO_2 concentration of 10% regardless of other conditions. At the same time, the effective access of water and CO_2 are both important to optimal carbonation. The impact of RH on the carbonation does not behave linearly but rather the RH of 78% outperformed all the other RH conditions within the scope of this work.

As for the hybrid reactive magnesia blended Portland cement (reactive magnesia, Portland cement, supplementary cementitious material like PFA or GGBFS), accelerated carbonation can promote the HCMs (hydrated magnesium carbonate such as dypingite, hydromagnesite, lansfordite, etc.,) and nesquehonite formation inside cement matrix and also improve the compressive strength compared with the atmospheric carbonation cured samples (Liska et al., 2008; Panesar and Mo, 2013). The natural carbonation on these mixes progresses very slowly even after more than 196 days of curing (Liska et al., 2008). The hybrid reactive magnesia blended Portland cement with substantial replacement of Portland cement with SCMs (as for PFA, > 50% PFA and > 25% reactive magnesia in mass ratio; as for GGBFS, PC:MgO:GGBFS = 1:2:2) can obtain equivalent or even better mechanical properties (e.g. compressive strength, toughness, stiffness) after enhanced carbonation curing (ambient temperature, ambient pressure but with > 20% CO_2 concentration, and longer aging duration) (Vandeperre and Al-Tabbaa, 2007; Panesar and Mo, 2013). This was attributed to the forced carbonation facilitating the formation of a denser matrix resulting from more nesquehonite *in-situ* formation from brucite which hence enhances the mechanical behavior and microstructure of reactive magnesia-aggregate systems (Liska et al., 2008). Water content (including original w/c ratio and relative humidity), CO_2 content, and porosity influence the carbonation efficiency even under enhanced carbonation conditions because these parameters control the diffusion of CO_2 into the cement matrix and the accessibility of water molecules to the intermediate magnesium bearing compounds (brucite, nesquehonite, hydrated magnesium carbonate). Maximum carbonation always takes place under moderate CO_2 concentration and medium relative humidity conditions (Vandeperre and Al-Tabbaa, 2007; Liska et al., 2008; Panesar and Mo, 2013).

Although the above carbonation experiment studies are relevant to ambient temperature and pressure conditions, the findings show us the high potentials of using reactive magnesia as one of the primary cementitious materials when we proceed with CO_2 geological sequestration and CO_2 EOR (enhanced oil recovery) operation due to: 1) mitigating the calcium leaching issues from Portland cement, 2) and the better performance as mechanical properties, permeability, and bonding strength derived from magnesium carbonates transformation (Shand, 2006b; Liska and Al-Tabbaa, 2012; Dung and Unluer, 2017; Ruan and Unluer, 2017). Therefore, other researchers have extended the investigations pertaining to high-temperature and high-pressure surroundings. Hänchen et al. (Hänchen et al., 2008) studied the supersaturation solution composed of $NaCO_3$ and $MgCl_2$ in equilibrium with CO_2. The nesquehonite, hydromagnesite, and magnesite would precipitate under the supersaturation conditions with respect to nesquehonite, brucite, and hydromagnesite respectively. Carbonation temperature and pressure dominate the type of precipitation. Nesquehonite would be formed with regards to the ambient condition (25°C, 1 bar of CO_2 partial pressure). Magnesite would be the final phase when the carbonation is cured at high-temperature (120°C) and no matter the CO_2 partial pressure. During these processes, hydromagnesite would be formed temporarily.

Frost et al. inspected the thermal stability of artinite [$MgCO_3{\cdot}Mg(OH)_2{\cdot}3H_2O$], dypingite [$4MgCO_3{\cdot}Mg(OH)_2{\cdot}5H_2O$], and brugnatellite ($MgCO_3{\cdot}2H_2O$) by use of the DTA method (Frost et al., 2008). The dehydration temperature for these three compounds is 219°C, 213°C, and 247°C respectively. In addition, the decarbonization temperature is within the range of 350°C–355°C. These results provide reference not only to the CO_2 geosequestration with magnesium-bearing minerals but to the reactive magnesia blended Portland cement studies.

Qakofu et al. studied the magnesite formation under low temperature (35°C and 50°C) and high CO_2 partial pressure (90 and 110 atm) conditions (Qafoku et al., 2015). They found that the formation of magnesite through an aqueous solution medium would progress very slowly even with the supercritical CO_2 phase. However, in the long-term view (56 days for 50°C case and 135 days for 35°C case), the intermediate nesquehonite and hydrated magnesium carbonate would transform into magnesite finally.

Srivastava et al. investigated the resistance performance of dead burnt magnesia (calcined at 1,250°C) incorporation into Class H oil well cement under high-temperature (107°C) and high-pressure (16.4 MPa, 41 MPa) conditions lasting for 14 days (Srivastava et al., 2018). Apart from the expansion effect, magnesia has the potential to improve the carbonic resistance of oil well cement sheath granted that the formulation of magnesia blended Portland cement should be designed with care to realize the synchronized hydration between magnesia and PC. In terms of carbonic acid resistance and degradation prevention of PC material, lower temperature and CO_2 partial pressure are both desired. However, from another viewpoint, these aging conditions would not favor the formation of magnesium-bearing carbonates.

7 CONCLUSION

Based on the review of recently published literature regarding research evolvement of magnesia blended Portland cement, several works have been done: 1) principal chemical property and category of Portland cement; 2) physical and chemical property of magnesia and its relationship with manufacturing technology; 3) differences between geotechnical well construction and civil construction regarding cement materials; 4) outline of typical characterization methods used in this research that provided significant validation on the alternation of physical-chemical-mechanical properties of magnesia blended PC materials under different conditions; 5) modeling study methods in terms of the correlation between the cementitious materials hydration, its volumetric variation, and the corresponding stress-strain and mechanical properties; 6) extraction of the previous studies' outcomes on hydration and expansion of magnesia blended PC; 7) summary of experimental investigation results of carbonation on magnesia cement and magnesia blended PC system. Whereby, it is evident that magnesia has the high potential to be used in Portland cement mix not only in respect of well integrity of geotechnical well construction (expansion, carbonation), but also in the light of greenhouse gas emission mitigation (lower energy consumption) and further carbon dioxide capture and utilization (carbonation). By the reasonable tuning among the characteristics of magnesia, the downhole surrounding conditions, and the formulation of the cement slurry, the incorporation of magnesia into PC can not only address/mitigate the micro-annulus issue but still improve the shear bonding strength at the cementing interfaces. In addition, compared with the conventional Portland cement sheath downhole suffered from the calcium leaching problem, the caustic magnesia introduction into Portland cement has a potential advantage over carbon dioxide geological sequestration well integrity because of the denser *in-situ* porous matrix evolvement, equivalent mechanical strength properties gain, and more stable carbon fixation features of magnesium carbonate. However, since the impact of magnesia on Portland cement strongly depended on its properties (calcination conditions, particle size, reactivity) and the aging conditions (downhole temperature, pressure, contacting medium), the extended research needs to be done in the future such as the synchronized hydration between magnesia and Portland cement, the dosage limit of caustic magnesia in Portland cement in respect of CO_2 sequestration and the corresponding mechanical properties analysis, and the hybrid mix (caustic magnesia, Portland cement, and other supplementary cementitious materials) targeting the co-existence of the geothermal and carbonic acid environment.

AUTHOR CONTRIBUTIONS

Conceptualization, WC Methodology, WC, SE Validation, MM, AAM Data curation, WC, AAM Writing—original draft preparation, WC Revision, WC, SE, MM, and AAM Supervision, WC.

ACKNOWLEDGMENTS

The authors would like to thank CPG (College of Petroleum Engineering and Geosciences) of KFUPM (King Fahd University of Petroleum and Minerals).

SUPPLEMENTARY MATERIAL

The Supplementary Material for this article can be found online at: https://www.frontiersin.org/articles/10.3389/fmats.2021.754431/full#supplementary-material

REFERENCES

Agofack, N. (2015). *Comportement des Ciments Pétroliers au Jeune âge et Intégrité des Puits. Ph.D. thesis*. Champs-sur-Marne, France: Université Paris-Est.

Agofack, N., Ghabezloo, S., Sulem, J., Garnier, A., and Urbanczyk, C. (2019). Onset of Creation of Residual Strain during the Hydration of Oil-Well Cement Paste. *Cement Concrete Res.* 116, 27–37. doi:10.1016/j.cemconres.2018.10.022

Al-Tabbaa, A. (2013). "19 - Reactive Magnesia Cement," in *Eco-Efficient Concrete*. Editors F. Pacheco-Torgal, S. Jalali, J. Labrincha, and V. John (Woodhead Publishing, Woodhead Publishing Series in Civil and Structural Engineering), 523–543. doi:10.1533/9780857098993.4.523

American Petroleum Institute (2002). "API Specification 10A - Specification for Cements and Materials for Well Cementing," in *API Standards Book* (American Petroleum Institute), 1–58. Standard.

American Petroleum Institute (2019). "API Specification 10A - Specification for Cements and Materials for Well Cementing," in *API Standards Book* (American Petroleum Institute), 1–76. Standard.

Aminu, M. D., Nabavi, S. A., Rochelle, C. A., and Manovic, V. (2017). A Review of Developments in Carbon Dioxide Storage. *Appl. Energ.* 208, 1389–1419. doi:10.1016/j.apenergy.2017.09.015

Aphane, M. E. (2007). *The Hydration of Magnesium Oxide with Different Reactivities by Water and Magnesium Acetate*. Pretoria, South Africa: Master's thesis, University of South Africa.

API (2013). *API RP 10B-2 Recommended Practice for Testing Well Cements*. Second Edition. Washington, DC: API Recommended Practice. 10B-2Standard.

API (2015). *ANSI/API RP 10B-5 Recommended Practice on Determination of Shrinkage and Expansion of Well Cement Formulations at Atmospheric Pressure*. . Washington, DC: ANSI/API RECOMMENDED PRACTICE. 10B-5. Standard.

Appah, D., and Reichetseder, P. (2002). Practical Improvements in CaO-Swelling Cements. *J. Pet. Sci. Eng.* 36, 61–70. doi:10.1016/s0920-4105(02)00251-6

ASTM International (2009). "ASTM C114-18 Standard Test Methods for Chemical Analysis of Hydraulic Cement," in ASTM Standard Book (West Conshohocken, PA: ASTM), 110–141. Standard. doi:10.1520/C0114-18.1.3

ASTM International (2019a). "ASTM C 150 - Standard Specification for Portland Cement," in ASTM Standard Book (West Conshohocken, PA: ASTM), 1–9. Standard. doi:10.1520/C0150

ASTM International (2019b). "ASTM C 465 - Standard Specification for Processing Additions for Use in the Manufacture of Hydraulic Cements," in ASTM Standard Book (West Conshohocken, PA: ASTM), 1–5. Standard. doi:10.1520/C0465-19

ASTM International (2020). *ASTM C109/C109M - Standard Test Method for Compressive Strength of Hydraulic Cement Mortars (Using 2-in. Or [50 Mm] Cube Specimens)*. West Conshohocken, PA: ASTM, 1–12. Standard. doi:10.1520/C0109M-20B

Backe, K. R., Lile, O. B., and Lyomov, S. K. (2001). Characterizing Curing Cement Slurries by Electrical Conductivity. *SPE Drilling & Completion.* 16, 207. doi:10.2118/74694-PA

Ball, M. C., and Taylor, H. F. W. (1961). The Dehydration of Brucite. *Mineral. Mag. J. Mineral. Soc.* 32, 754–766. doi:10.1180/minmag.1961.032.253.02

Ballirano, P., De Vito, C., Ferrini, V., and Mignardi, S. (2010). The Thermal Behaviour and Structural Stability of Nesquehonite, $MgCO_3{\cdot}3H_2O$, Evaluated by *In Situ* Laboratory Parallel-Beam X-ray Powder Diffraction: New Constraints on CO_2 Sequestration Within Minerals. *J. Hazard. Mater.* 178, 522–528. doi:10.1016/j.jhazmat.2010.01.113

Barnes, P., and Bensted, J. (2002). *Structure and Performance of Cements*. Second Edition. London, United Kingdom: Taylor & Francis. doi:10.1201/9781482295016

Baumgarte, C., and Thiercelin, M. (1999). "Case Studies of Expanding Cement to Prevent Microannular Formation," in SPE Annual Technical Conference and Exhibition (Houston, Texas: Society of Petroleum Engineers). doi:10.2118/56535-MS

Béarat, H., McKelvy, M. J., Chizmeshya, A. V. G., Sharma, R., and Carpenter, R. W. (2002). Magnesium Hydroxide Dehydroxylation/Carbonation Reaction Processes: Implications for Carbon Dioxide Mineral Sequestration. *J. Am. Ceram. Soc.* 85, 742–748. doi:10.1111/j.1151-2916.2002.tb00166.x

Bentur, A., Igarashi, S.-i., and Kovler, K. (2001). Prevention of Autogenous Shrinkage in High-Strength Concrete by Internal Curing Using Wet Lightweight Aggregates. *Cement Concrete Res.* 31, 1587–1591. doi:10.1016/S0008-8846(01)00608-1

Biernacki, J. J., Bullard, J. W., Sant, G., Brown, K., Glasser, F., Jones, S., et al. (2017). Cements in the 21st Century: Challenges, Perspectives, and Opportunities. *J. Am. Ceram. Soc.* 100, 2746–2773. doi:10.1111/jace.14948

Blezard, R. G. (1998). "Reflections on the History of the Chemistry of Cement," in Construction Materials Group of the Society of Chemical Industry (SCI) (London: Society of Chemical Industry), 1–27.

Bois, A.-P., Vu, M.-H., Noël, K., Badalamenti, A., Delabroy, L., Thérond, E., et al. (2019). Evaluating Cement-Plug Mechanical and Hydraulic Integrity. *SPE Drilling & Completion.* 34, 92–102. doi:10.2118/191335-PA

Brandl, A., Valentino, V., Fauchille, G., Thein, A., Stanley, R., Rivera, N. N., et al. (2014). "Successful History of Cementing and Zonal Isolation in Thailand's High Temperature Offshore Wells," in Abu Dhabi International Petroleum Exhibition and Conference (Abu Dhabi: UAE, Society of Petroleum Engineers). doi:10.2118/172125-ms

Brindley, G. W., and Hayami, R. (1963). Kinetics and Mechanisms of Dehydration and Recrystallization of Serpentine—I. *Clays and Clay Minerals.* 12, 35–47. doi:10.1346/ccmn.1963.0120107

Britannica (2019). Micrometer. Available at: https://www.britannica.com/technology/micrometer (Accessed September 15, 2020).

Cao, F., Miao, M., and Yan, P. (2018a). Effects of Reactivity of MgO Expansive Agent on its Performance in Cement-Based Materials and an Improvement of the Evaluating Method of MEA Reactivity. *Construction Building Mater.* 187, 257–266. doi:10.1016/j.conbuildmat.2018.07.198

Cao, F., Miao, M., and Yan, P. (2018b). Hydration Characteristics and Expansive Mechanism of MgO Expansive Agents. *Construction Building Mater.* 183, 234–242. doi:10.1016/j.conbuildmat.2018.06.164

Chatelier, H., and Mack, J. (1905). *Experimental Researches on the Constitution of Hydraulic Mortars*. London, United Kingdom: McGraw Publishing Company.

Chen, H., Wyrzykowski, M., Scrivener, K., and Lura, P. (2013). Prediction of Self-Desiccation in Low Water-To-Cement Ratio Pastes Based on Pore Structure Evolution. *Cement Concrete Res.* 49, 38–47. doi:10.1016/j.cemconres.2013.03.013

Crippa, M., Oreggioni, D., Muntean, M., Schaaf, E., Lo Vullo, E., Solazzo, E., et al. (2017). *Fossil CO_2 and GHG Emissions of All World Countries - 2019 Report*. Brussels, Belgium: Germany: European Commission.

Curry, K. C., and van Oss, H. G. (2017). *USGS 2017 minerals Yearbook - Cement (Advance Release)*. Washington, DC: United States: USGS.

Davies, P. J., and Bubela, B. (1973). The Transformation of Nesquehonite into Hydromagnesite. *Chem. Geology.* 12, 289–300. doi:10.1016/0009-2541(73)90006-5

Doerner, H. A., Fortner, O. W., and Holbrook, W. F. (1946). *The Bicarbonate Process for the Production of Magnesium Oxide*. Washington, D.C: Technical paper/United States. Bureau of Mines;684U.S. Govt. Print. Off., Bureau of Mines.

Dung, N. T., and Unluer, C. (2016). Improving the Performance of Reactive MgO Cement-Based Concrete Mixes. *Construction Building Mater.* 126, 747–758. doi:10.1016/j.conbuildmat.2016.09.090

Dung, N. T., and Unluer, C. (2017). Sequestration of CO_2 in Reactive MgO Cement-Based Mixes With Enhanced Hydration Mechanisms. *Construction Building Mater.* 143, 71–82. doi:10.1016/j.conbuildmat.2017.03.038

Fernández, A., Chimenos, J., Segarra, M., Fernández, M., and Espiell, F. (1999). Kinetic Study of Carbonation of MgO Slurries. *Hydrometallurgy.* 53, 155–167. doi:10.1016/S0304-386X(99)00039-0

Frederick, M. L., and Thomas, O. M. (2020). Cement. Available at: https://www.britannica.com/technology/cement-building-material (Accessed December 12, 2020).

Frost, R. L., Bahfenne, S., Graham, J., and Martens, W. N. (2008). Thermal Stability of Artinite, Dypingite and Brugnatellite — Implications for the Geosequestration of Green House Gases. *Thermochim. Acta.* 475, 39–43. doi:10.1016/j.tca.2008.06.007

Fruhwirth, O., Herzog, G., Hollerer, I., and Rachetti, A. (1985). Dissolution and Hydration Kinetics of MgO. *Surf. Technology.* 24, 301–317. doi:10.1016/0376-4583(85)90080-9

Ghofrani, R., and Plack, H. (1993). "CaO-and/or MgO-Swelling Cements: a Key for Providing a Better Annular Sealing?" in SPE/IADC Drilling Conference (Amsterdam, Netherlands: Society of Petroleum Engineers), 199–214. doi:10.2118/25697-MS

Goodman, J. F., and Bowden, F. P. (1958). The Decomposition of Magnesium Hydroxide in an Electron Microscope. *Proc. R. Soc. Lond. Ser. A. Math. Phys. Sci.* 247, 346–352. doi:10.1098/rspa.1958.0188

Gowida, A. H., Ahmad, Z., Elkatatny, S., and Mahmoud, M. (2018). "Cement Evaluation Challenges," in SPE Kingdom of Saudi Arabia Annual Technical Symposium and Exhibition, Dammam (Saudi Arabia: Society of Petroleum Engineers). doi:10.2118/192360-MS

Gregg, S. J., Packer, R. K., and Wheatley, K. H. (1955). The Production of Active Solids by Thermal Decomposition. Part V. The Sintering of Active Magnesium Oxide. *J. Chem. Soc.* 30, 46–50. doi:10.1039/JR9550000046

Guren, M. G., Sveinsson, H. A., Hafreager, A., Jamtveit, B., Malthe-Sørenssen, A., and Renard, F. (2021). Molecular Dynamics Study of Confined Water in the Periclase-Brucite System Under Conditions of Reaction-Induced Fracturing. *Geochimica et Cosmochimica Acta.* 294, 13–27. doi:10.1016/j.gca.2020.11.016

Gutteridg, W. A., and Pomeroy, C. D. (1983). Cement in its Conventional Uses: Problems and Possibilities [and Discussion]. *Philosophical Trans. R. Soc. Lond. Ser. A, Math. Phys. Sci.* 310, 7–15. doi:10.1098/rsta.1983.0061

Hammad, M. A. A., and Altameini, Y. M. (2002). "Cement Matrix Evaluation," in IADC/SPE Asia Pacific Drilling Technology (Jakarta, Indonesia: Society of Petroleum Engineers). doi:10.2118/77213-MS

Hänchen, M., Prigiobbe, V., Baciocchi, R., and Mazzotti, M. (2008). Precipitation in the Mg-Carbonate System— Effects of Temperature and CO_2 Pressure. *Chem. Eng. Sci.* 63, 1012–1028. doi:10.1016/j.ces.2007.09.052

Hashimoto, H., Komaki, E., Hayashi, F., and Uematsu, T. (1980). Partial Decomposition of Dolomite in CO_2. *J. Solid State. Chem.* 33, 181–188. doi:10.1016/0022-4596(80)90118-8

Hopkinson, L., Rutt, K., and Cressey, G. (2008). The Transformation of Nesquehonite to Hydromagnesite in the System $CaO \cdot MgO \cdot H_2O \cdot CO_2$: An Experimental Spectroscopic Study. *J. Geology.* 116, 387–400. doi:10.1086/588834

Huajun, C., Sudong, H., Qisheng, W., Changsen, Z., and Tao, Y. (2013). Effect of MgO Expanding Agent on Early Performance of Oil Well Cement under Three Dimensional Constraint. *J. China Univ. Pet. (Zirankexueban).* 37, 153–158. doi:10.3969/j.issn.1673-5005.2013.06.025

ISO (2004). *Petroleum and Natural Gas Industries — Cements and Materials for Well Cementing — Part 5: Determination of Shrinkage and Expansion of Well Cement Formulations at Atmospheric Pressure*. ISO 10426-5:2004. Standard. Geneva, Switzerland: International Organization for Standardization.

Jafariesfad, N., Geiker, M. R., Gong, Y., Skalle, P., Zhang, Z., and He, J. (2017a). Cement Sheath Modification Using Nanomaterials for Long-Term Zonal Isolation of Oil Wells: Review. *J. Pet. Sci. Eng.* 156, 662–672. doi:10.1016/j.petrol.2017.06.047

Jafariesfad, N., Geiker, M. R., and Skalle, P. (2017b). Nanosized Magnesium Oxide With Engineered Expansive Property for Enhanced Cement-System Performance. *SPE J.* 22, 1681–1689. doi:10.2118/180038-PA

Jafariesfad, N., Gong, Y., Geiker, M. R., and Skalle, P. (2016). "Nano-Sized MgO With Engineered Expansive Property for Oil Well Cement Systems," in SPE Bergen One Day Seminar (Bergen: Society of Petroleum Engineers). doi:10.2118/180038-MS

Jafariesfad, N., Sangesland, S., Gawel, K., and Torsæter, M. (2020). New Materials and Technologies for Life-Lasting Cement Sheath: A Review of Recent Advances. *SPE Drilling & Completion.* 35, 262–278. doi:10.2118/199885-PA

Jin, F., and Al-Tabbaa, A. (2020). "Magnesia in Alkali Activated Cements," in *Magnesia Cements*. Editors M. A. Shand, A. Al-Tabbaa, J. Qian, L. Mo, and F. Jin (Oxford: Elsevier), 213–241. doi:10.1016/B978-0-12-391925-0.00015-7

Johnston, S. (1990). The Evolution of FTIR Technology. *Chem. Britain.* 26, 573–579. doi:10.1002/chin.199044381

José, N., Ahmed, H., Miguel, B., Luís, E., and Jorge, d. B. (2020). Magnesia (MgO) Production and Characterization, and its Influence on the Performance of Cementitious Materials: A Review. *Materials.* 13, 4752. doi:10.3390/ma13214752

Jung, K. S., Keener, T. C., Green, V. C., and Khang, S.-J. (2004). CO_2 Absorption Study in a Bubble Column Reactor With $Mg(OH)_2$. *Int. J. Environ. Technology Management.* 4, 116–136. doi:10.1504/ijetm.2004.004625

Justnes, H., Reynier, B., van Loo, D., and Sellevold, E. J. (1994). An Evaluation of Methods for Measuring Chemical Shrinkage of Cementitious Pastes. *Nordic Concrete Res.* 14, 45–61.

Justnes, H., van Loo, D., Reyniers, B., Skalle, P., Sveen, J., and Sellevold, E. J. (1995). Chemical Shrinkage of Oil Well Cement Slurries. *Adv. Cement Res.* 7, 85–90. doi:10.1680/adcr.1995.7.26.85

Khan, S. A., Khan, S. B., Khan, L. U., Farooq, A., Akhtar, K., and Asiri, A. M. (2018). *Fourier Transform Infrared Spectroscopy: Fundamentals and Application in Functional Groups and Nanomaterials Characterization*. Cham: Springer International Publishing, 317–344. doi:10.1007/978-3-319-92955-2_9

Khangaonkar, P., Othman, R., and Ranjitham, M. (1990). Studies on Particle Breakage During Hydration of Calcined Magnesite. *Minerals Eng.* 3, 227–235. doi:10.1016/0892-6875(90)90095-S

Knibbs, N. (1924). *Lime and Magnesia: The Chemistry, Manufacture and Uses of the Oxides, Hydroxides and Carbonates of Calcium and Magnesium*. New York, NY: D. Van Nostrand Company.

Langmuir, D. (1965). Stability of Carbonates in the System $MgO\text{-}CO_2\text{-}H_2O$. *J. Geology.* 73, 730–754. doi:10.1086/627113

Lawrence, C. D. (1998). "4 - the Constitution and Specification of Portland Cements," in *Lea's Chemistry of Cement and Concrete*. Editor P. C. Hewlett Fourth Edition (Oxford: Butterworth-Heinemann), 131–193. doi:10.1016/b978-075066256-7/50016-3

Lehne, J., and Preston, F. (2017). *Making Concrete Change - Innovation in Low-Carbon Cement and Concrete*. United States: Chatham House.

Li, F., Chen, Y., Long, S., Wang, B., and Li, G. (2010). Research on the Preparation and Properties of MgO Expansive Agent. *Adv. Cement Res.* 22, 37–44. doi:10.1680/adcr.2008.22.1.37

LibreTexts (2019). Calorimetry. Available at: https://chem.libretexts.org/@go/page/157956 (Accessed February 22, 2021).

Liska, M., and Al-Tabbaa, A. (2009). Ultra-Green Construction: Reactive Magnesia Masonry Products. *Proc. Inst. Civil Eng. - Waste Resource Management.* 162, 185–196. doi:10.1680/warm.2009.162.4.185

Liska, M., and Al-Tabbaa, A. (2012). Performance of Magnesia Cements in Porous Blocks in Acid and Magnesium Environments. *Adv. Cement Res.* 24, 221–232. doi:10.1680/adcr.11.00011

Liska, M., Vandeperre, L. J., and Al-Tabbaa, A. (2008). Influence of Carbonation on the Properties of Reactive Magnesia Cement-Based Pressed Masonry Units. *Adv. Cement Res.* 20, 53–64. doi:10.1680/adcr.2008.20.2.53

Liu, C., Wang, D., Zheng, H., and Liu, T. (2017). A Dehydroxylation Kinetics Study of Brucite $Mg(OH)_2$ at Elevated Pressure and Temperature. *Phys. Chem. Minerals.* 44, 297–306. doi:10.1007/s00269-016-0857-y

Lura, P., and Jensen, O. M. (2007). Measuring Techniques for Autogenous Strain of Cement Paste. *Mater. Structures.* 40, 431–440. doi:10.1617/s11527-006-9180-2

Lura, P., Jensen, O. M., and van Breugel, K. (2003). Autogenous Shrinkage in High-Performance Cement Paste: An Evaluation of Basic Mechanisms. *Cement Concrete Res.* 33, 223–232. doi:10.1016/S0008-8846(02)00890-6

Mao, W., Litina, C., and Al-Tabbaa, A. (2020). Development and Application of Novel Sodium Silicate Microcapsule-Based Self-Healing Oil Well Cement. *Materials.* 13, 456. doi:10.3390/ma13020456

Maravelaki-Kalaitzaki, P., and Moraitou, G. (1999). Sorel's Cement Mortars: Decay Susceptibility and Effect on Pentelic Marble. *Cement Concrete Res.* 29, 1929–1935. doi:10.1016/S0008-8846(99)00197-0

Michaux, M., Nelson, E., and Vidick, B. (1989). Cement Chemistry and Additives. *Oilfiled Rev. Schulumberger.* 1, 7–12.

Mitchell, A. E. (1923). CXX. — Studies on the Dolomite System. Part I. The Nature of Dolomite. *J. Chem. Soc. Trans.* 123, 1055–1069. doi:10.1039/CT9232301055

Mo, L., and Al-Tabbaa, A. (2020). "Magnesia as an Expansive Additive," in *Magnesia Cements*. Editors M. A. Shand, A. Al-Tabbaa, J. Qian, L. Mo, and F. Jin (Oxford: Elsevier), 243–274. doi:10.1016/B978-0-12-391925-0.00016-9

Mo, L., Deng, M., Tang, M., and Al-Tabbaa, A. (2014). MgO Expansive Cement and Concrete in China: Past, Present and Future. *Cement Concrete Res.* 57, 1–12. doi:10.1016/j.cemconres.2013.12.007

Mo, L., Deng, M., and Tang, M. (2010). Effects of Calcination Condition on Expansion Property of MgO-Type Expansive Agent Used in Cement-Based Materials. *Cement Concrete Res.* 40, 437–446. doi:10.1016/j.cemconres.2009.09.025

Mo, L., Liu, M., Al-Tabbaa, A., and Deng, M. (2015). Deformation and Mechanical Properties of the Expansive Cements Produced by Inter-Grinding Cement Clinker and MgOs With Various Reactivities. *Construction Building Mater.* 80, 1–8. doi:10.1016/j.conbuildmat.2015.01.066

Mo, L., and Panesar, D. K. (2012). Effects of Accelerated Carbonation on the Microstructure of Portland Cement Pastes Containing Reactive MgO. *Cement Concrete Res.* 42, 769–777. doi:10.1016/j.cemconres.2012.02.017

Moradpour, R., Taheri-Nassaj, E., Parhizkar, T., and Ghodsian, M. (2013). The Effects of Nanoscale Expansive Agents on the Mechanical Properties of Non-Shrink Cement-Based Composites: The Influence of Nano-MgO Addition. *Composites B: Eng.* 55, 193–202. doi:10.1016/j.compositesb.2013.06.033

Murtaza, M., Mahmoud, M., Elkatatny, S., Majed, A. A., Chen, W., and Jamaluddin, A. (2019). *Experimental Investigation of the Impact of Modified Nano Clay on the Rheology of Oil Well Cement Slurry* in vol. Day 1 Tue, March 26, 2019 of IPTC International Petroleum Technology Conference. doi:10.2523/IPTC-19456-MS.D011S014R004

Nagataki, S., and Gomi, H. (1998). Expansive Admixtures (Mainly Ettringite). *Cement and Concrete Composites.* 20, 163–170. doi:10.1016/s0958-9465(97)00064-4

Nelson, E. B., and Guillot, D. (2006). "Introduction," in *Well Cementing*. Editors E. B. Nelson and D. Guillot (Schlumberger), 9–12.

Nelson, E. B., and Drecq, P. (1990). "7 Special Cement Systems," in *Well CementingDevelopments in Petroleum Science*. Editor E. B. Nelson (Elsevier), 7–1–7–14. doi:10.1016/S0376-7361(09)70305-X

Neville, A., and Neville, A. (2011). *Properties of Concrete*. London, United Kingdom: Pearson.

Ochs, D., Brause, M., Braun, B., Maus-Friedrichs, W., and Kempter, V. (1998). CO_2 Chemisorption at Mg and MgO Surfaces: A Study With MIES and UPS (He I). *Surf. Sci.* 397, 101–107. doi:10.1016/S0039-6028(97)00722-X

Ogawa, K., and Roy, D. M. (1981). C_4A_3S Hydration Ettringite Formation, and its Expansion Mechanism: I. Expansion; Ettringite Stability. *Cement Concrete Res.* 11, 741–750. doi:10.1016/0008-8846(81)90032-6

Ogawa, K., and Roy, D. M. (1982). C_4A_3S Hydration, Ettringite Formation, and its Expansion Mechanism: II. Microstructural Observation of Expansion. *Cement Concrete Res.* 12, 101–109. doi:10.1016/0008-8846(82)90104-1

Olivier, J., and Peters, J. (2017). *Trends in Global CO_2 and Total Greenhouse Gas Emissions - 2019 Report*. Netherlands: PBL Netherlands Environmental Assessment Agency.

Omidi, M., Fatehinya, A., Farahani, M., Akbari, Z., Shahmoradi, S., Yazdian, F., et al. (2017). "7 - Characterization of Biomaterials," in *Biomaterials for Oral and Dental Tissue Engineering*. Editors L. Tayebi and K. Moharamzadeh (Woodhead Publishing), 97–115. doi:10.1016/B978-0-08-100961-1.00007-4

Onaisi, A., Urbanczyk, C., Lansot, J.-Y., and Garnier, A. (2017). "Impact of Poro-Chemo-Mechanical Parameters on Pre-Stress and Cement Sheath Integrity Under Well Pressure and Thermal Loadings," in Abu Dhabi International Petroleum Exhibition & Conference (Abu Dhabi: UAE, 2017 (Society of Petroleum Engineers). doi:10.2118/188761-MS.D041S116R002

Onaisi, A., Zinsmeister, L., Urbanczyk, C., Garnier, A., and Lansot, J.-Y. (2019). "Is Post Expansion Measured by Standard Ring Experiment Meaningful for Cement Sheath Integrity?" in Abu Dhabi International Petroleum Exhibition and Conference 2018, ADIPEC 2018 (Abu Dhabi: Society of Petroleum Engineers). doi:10.2118/192718-MS

Onishi, H., Egawa, C., Aruga, T., and Iwasawa, Y. (1987). Adsorption of Na Atoms and Oxygen-Containing Molecules on MgO(100) and (111) Surfaces. *Surf. Sci.* 191, 479–491. doi:10.1016/S0039-6028(87)81192-5

Panesar, D. K., and Mo, L. (2013). Properties of Binary and Ternary Reactive MgO Mortar Blends Subjected to CO_2 Curing. *Cement and Concrete Composites.* 38, 40–49. doi:10.1016/j.cemconcomp.2013.03.009

Parcevaux, P. A., and Sault, P. H. (1984). "Cement Shrinkage and Elasticity: A New Approach for a Good Zonal Isolation," in SPE Annual Technical Conference and Exhibition (Houston, Texas: Society of Petroleum Engineers). doi:10.2118/13176-ms

Patel, H., Salehi, S., and Teodoriu, C. (2019). "Assessing Mechanical Integrity of Expanding Cement," in SPE Oklahoma City Oil and Gas Symposium/Production and Operations Symposium (Oklahoma City, Oklahoma, USA. doi:10.2118/195225-ms

Pearce, F. (1997). The Concrete Jungle Overheats. Available at: https://www.newscientist.com/article/mg15520912-200-the-concrete-jungle-overheats/(Accessed January 03, 2021).

Peng, X., and Barteau, M. (1990). Characterization of Oxide Layers on Mg (0001) and Comparison of H_2O Adsorption on Surface and Bulk Oxides. *Surf. Sci.* 233, 283–292. doi:10.1016/0039-6028(90)90641-k

Piot, B. (2020). Cement and Cementing: An Old Technique with a Future? Available at: https://www.spe.org/dl/docs/2009/Piot.pdf (Accessed August 03, 2019).

Poole, A., and Sims, I. (2016). *Concrete Petrography: A Handbook of Investigative Techniques*. Second Edition. Boca Raton, FL: CRC Press.

Qafoku, O., Dixon, D. A., Rosso, K. M., Schaef, H. T., Bowden, M. E., Arey, B. W., et al. (2015). Dynamics of Magnesite Formation at Low Temperature and High pCO_2 in Aqueous Solution. *Environ. Sci. Technology.* 49, 10736–10744. doi:10.1021/acs.est.5b02588

Qureshi, T. S., Kanellopoulos, A., and Al-Tabbaa, A. (2016). Encapsulation of Expansive Powder Minerals Within a Concentric Glass Capsule System for Self-Healing Concrete. *Construction Building Mater.* 121, 629–643. doi:10.1016/j.conbuildmat.2016.06.030

Ramachandran, V., and Feldman, R. F. (1996). "1 - Concrete Science," in *Concrete Admixtures Handbook*. Editor V. Ramachandran (Park Ridge, NJ: William Andrew Publishing), 1–66. doi:10.1016/b978-081551373-5.50005-2

Rao, P. P., Sutton, D. L., Childs, J. D., and Cunningham, W. C. (1982). An Ultrasonic Device for Nondestructive Testing of Oilwell Cements at Elevated Temperatures and Pressures. *J. Pet. Technology.* 34, 2611–2616. doi:10.2118/9283-PA

Raval, N., Maheshwari, R., Kalyane, D., Youngren-Ortiz, S. R., Chougule, M. B., and Tekade, R. K. (2019). "Chapter 10 - Importance of Physicochemical Characterization of Nanoparticles in Pharmaceutical Product Development," in *Basic Fundamentals of Drug Delivery*. Editor R. K. Tekade (Academic Press, Advances in Pharmaceutical Product Development and Research), 369–400. doi:10.1016/b978-0-12-817909-3.00010-8

Ravi, K., Bosma, M., and Gastebled, O. (2002). "Improve the Economics of Oil and Gas Wells by Reducing the Risk of Cement Failure," in IADC/SPE Drilling Conference (Dallas, Texas: Society of Petroleum Engineers), 377–389. doi:10.2118/74497-ms

Reddy, B. R., Xu, Y., Ravi, K., Gray, D. W., and Pattillo, P. (2009). Cement Shrinkage Measurement in Oilwell Cementing - A Comparative Study of Laboratory Methods and Procedures. *SPE Drilling & Completion.* 24, 104–114. doi:10.2118/103610-pa

Ridha, S., Irawan, S., and Ariwahjoedi, B. (2013). Strength Prediction of Class G Oilwell Cement During Early Ages by Electrical Conductivity. *J. Pet. Exploration Prod. Technology.* 3, 303–311. doi:10.1007/s13202-013-0075-9

Rodgers, L. (2018). Climate Change: The Massive CO_2 Emitter You May Not Know About. Available at: http://www-personal.umich.edu/~mejn/netdata/(Accessed January 03, 2021).

Rogers, M. J., Dillenbeck, R. L., and Eid, R. N. (2005). Transition Time of Cement Slurries. *J. Pet. Technology.* 57, 45–47. doi:10.2118/0805-0045-jpt

Rogers, M. J., Dillenbeck, R. L., and Eid, R. N. (2004). "Transition Time of Cement Slurries, Definitions and Misconceptions, Related to Annular Fluid Migration," in SPE Annual Technical Conference and Exhibition (Houston: Society of Petroleum Engineers), 3987–4000. doi:10.2118/90829-MS

Rothon, R., and Hornsby, P. (2014). "Chapter 9 - Fire Retardant Fillers for Polymers," in *Polymer Green Flame Retardants*. Editors C. D. Papaspyrides and P. Kiliaris (Amsterdam: Elsevier), 289–321. doi:10.1016/B978-0-444-53808-6.00009-3

Ruan, S., and Unluer, C. (2017). Influence of Mix Design on the Carbonation, Mechanical Properties and Microstructure of Reactive MgO Cement-Based Concrete. *Cement and Concrete Composites.* 80, 104–114. doi:10.1016/j.cemconcomp.2017.03.004

Rubiandini, R., Siregar, S., Suhascaryo, N., and Efrial, D. (2005). The Effect of CaO and MgO as Expanding Additives to Improve Cement Isolation Strength Under HPHT Exposure. *J. Eng. Technol. Sci.* 37, 29–48. doi:10.5614/itbj.eng.sci.2005.37.1.3

Samudio, M. (2017). *Modelling of an Oil Well Cement Paste from Early Age to Hardened State : Hydration Kinetics and Poromechanical Behaviour*. Champs-sur-Marne, France: Thesis, Université Paris-Est.

Sant, G., Lura, P., and Weiss, W. J. (2006). Measurement of Volume Change in Cementitious Materials at Early Ages: Review of Testing Protocols and Interpretation of Results. *Transportation Res. Rec. J. Transportation Res. Board.* 1979, 21–29. doi:10.1177/0361198106197900104

Scrivener, K., Snellings, R., and Lothenbach, B. (2016). *A Practical Guide to Microstructural Analysis of Cementitious Materials*. 1st ed. Place, UK: CRC Press. doi:10.1201/b19074

Shadravan, A., Schubert, J., Amani, M., and Teodoriu, C. (2014). "HPHT Cement Sheath Integrity Evaluation Method for Unconventional Wells," in SPE International Conference on Health, Safety, and Environment, Long Beach, California (California, USA: Society of Petroleum Engineers). doi:10.2118/168321-ms

Shahriar, A., and Nehdi, M. L. (2012). Rheological Properties of Oil Well Cement Slurries. *Proc. Inst. Civil Eng. - Construction Mater.* 165, 25–44. doi:10.1680/coma.2012.165.1.25

Shakirah, S. (2008). "A New Approach for Optimizing Cement Design to Eliminate Microannulus in Steam Injection Wells," in International Petroleum Technology Conference held in Kuala Lumpur (Malaysia: Society of Petroleum Engineers). doi:10.2523/IPTC-12407-MS

Shand, M. A. (2006a). *Calcination of Magnesium Hydroxide and Carbonate*. Hoboken, NJ: John Wiley & Sons, 83–96. doi:10.1002/0471980579.ch5

Shand, M. A. (2006b). *Environmental Applications*. Hoboken, NJ: John Wiley & Sons, 189–199. doi:10.1002/0471980579.ch12

Shand, M. A. (2006c). *Formation and Occurrence of Magnesite and Brucite*. Hoboken, NJ: John Wiley & Sons, 5–37. doi:10.1002/0471980579.ch2

Shand, M. A. (2006d). *Magnesia Cements*. Hoboken, NJ: John Wiley & Sons, 231–239. doi:10.1002/0471980579.ch16

Shand, M. A. (2006e). *Other Magnesia Products*. Hoboken, NJ: John Wiley & Sons, 133–154. doi:10.1002/0471980579.ch9

Shand, M. A. (2006f). *Physical and Chemical Properties of Magnesium Oxide*. Hoboken, NJ: John Wiley & Sons, 121–131. doi:10.1002/0471980579.ch8

Shand, M. A., and Jin, F. (2020). "Introduction – Characterization of MgO," in *Magnesia Cements*. Editors M. A. Shand, A. Al-Tabbaa, J. Qian, L. Mo, and F. Jin (Oxford: Elsevier), 1. doi:10.1016/B978-0-12-391925-0.00006-6

Sheila, D., Sankaran, C., and Khangaonkar, P. (1991). Studies on the Extraction of Magnesia from Low Grade Magnesites by Carbon Dioxide Pressure Leaching of Hydrated Magnesia. *Minerals Eng.* 4, 79–88. doi:10.1016/0892-6875(91)90120-k

Sherir, M. A. A., Hossain, K. M. A., and Lachemi, M. (2017). The Influence of MgO-Type Expansive Agent Incorporated in Self-Healing System of Engineered Cementitious Composites. *Construction Building Mater.* 149, 164–185. doi:10.1016/j.conbuildmat.2017.05.109

Sherir, M. A., Hossain, K. M., and Lachemi, M. (2016). Self-Healing and Expansion Characteristics of Cementitious Composites With High Volume Fly Ash and MgO-type Expansive Agent. *Construction Building Mater.* 127, 80–92. doi:10.1016/j.conbuildmat.2016.09.125

Silva, P. D., Bucea, L., and Sirivivatnanon, V. (2009). Chemical, Microstructural and Strength Development of Calcium and Magnesium Carbonate Binders. *Cement Concrete Res.* 39, 460–465. doi:10.1016/j.cemconres.2009.02.003

Sima, F., Ristoscu, C., Duta, L., Gallet, O., Anselme, K., and Mihailescu, I. (2016). "3 - Laser Thin Films Deposition and Characterization for Biomedical Applications," in Laser Surface Modification of Biomaterials. Editor R. Vilar (Woodhead Publishing), 77–125. doi:10.1016/B978-0-08-100883-6.00003-4

Simon, A. H. (2018). "Chapter 7 - Sputter Processing," in *Handbook of Thin Film Deposition*. Editors K. Seshan and D. Schepis (William Andrew Publishing), 195–230. doi:10.1016/b978-0-12-812311-9.00007-4

Smith, B. C. (2011). *Fundamentals of Fourier Transform Infrared Spectroscopy*. 2nd ed.. Boca Raton, FL: CRC Press. doi:10.1201/b10777

Smithson, G. L., and Bakhshi, N. N. (1969). The Kinetics and Mechanism of the Hydration of Magnesium Oxide in a Batch Reactor. *Can. J. Chem. Eng.* 47, 508–513. doi:10.1002/cjce.5450470602

Soroka, I. (1979). *Chapter 1 - Chemical and Mineralogical Composition*. London: Macmillan Education UK, 1–27. doi:10.1007/978-1-349-03994-4_1

Sorre, C. A., and Armstrong, C. R. (1976). Reactions and Equilibria in Magnesium Oxychloride Cements. *J. Am. Ceram. Soc.* 59, 51–54. doi:10.1111/j.1151-2916.1976.tb09387.x

Srivastava, A., Ahmed, R., and Shah, S. (2018). Effects of Magnesium Oxide on Carbonic Acid Resistance of Oil Well Cement. *J. Pet. Sci. Eng.* 170, 218–230. doi:10.1016/j.petrol.2018.06.059

Stiles, D. (2006). "Annular Formation Fluid Migration," in *Well Cementing*. Editors E. B. Nelson and D. Guillot (Schlumberger), 289–318.

Suhascaryo, N., Rubiandini, R. R., Siregar, S., and Nawangsidi, D. (2005). "The Effect of Expanding Additives to Improve Cement Isolation Strength to 250°C and 2000 Psi Conditions," in Proceedings World Geothermal Congress 2005 (Antalya), 29–47.

Sushko, P. V., Gavartin, J. L., and Shluger, A. L. (2002). Electronic Properties of Structural Defects at the MgO (001) Surface. *The J. Phys. Chem. B.* 106, 2269–2276. doi:10.1021/jp0129481

Tao, C., Kutchko, B. G., Rosenbaum, E., Wu, W.-T., and Massoudi, M. (2019). Steady Flow of a Cement Slurry. *Energies.* 12, 2604. doi:10.3390/en12132604

Temiz, H., Kantarci, F., and Emin Inceer, M. (2015). Influence of Blast-Furnace Slag on Behaviour of Dolomite Used as a Raw Material of MgO-type Expansive Agent. *Construction Building Mater.* 94, 528–535. doi:10.1016/j.conbuildmat.2015.07.059

ThermoScientific (2020). Introduction to Fourier Transform Infrared Spectroscopy. Available at: https://tools.thermofisher.com/content/sfs/brochures/BR50555_E_0513M_H_1.pdf (Accessed March 03, 2020).

Thiercelin, M. (2006). "Mechanical Properties of Well Cements," in *Well Cementing*. Editors E. B. Nelson and D. Guillot (Schlumberger), 269–288.

Thomas, J., Musso, S., Catheline, S., Chougnet-Sirapian, A., and Allouche, M. (2014a). "Expanding Cement for Improved Wellbore Sealing: Prestress Development, Physical Properties, and Logging Response," in SPE Deepwater Drilling and Completions Conference (Galveston: Society of Petroleum Engineers), 506–515. doi:10.2118/170306-ms

Thomas, J. J., Musso, S., and Prestini, I. (2014b). Kinetics and Activation Energy of Magnesium Oxide Hydration. *J. Am. Ceram. Soc.* 97, 275–282. doi:10.1111/jace.12661

Trout, E. A. (2019). "1 - the History of Calcareous Cements," in *Lea's Chemistry of Cement and Concrete*. Editors P. C. Hewlett and L. Martin (Butterworth-Heinemann), 1–29. doi:10.1016/b978-0-08-100773-0.00001-0

UNESCO (2021). Göbekli Tepe - World Heritage ListAvailable at: \url{https://whc.unesco.org/en/list/1572/ (Accessed June 1, 2011)

Unluer, C., and Al-Tabbaa, A. (2014). Enhancing the Carbonation of MgO Cement Porous Blocks Through Improved Curing Conditions. *Cement Concrete Res.* 59, 55–65. doi:10.1016/j.cemconres.2014.02.005

Unluer, C., and Al-Tabbaa, A. (2013). Impact of Hydrated Magnesium Carbonate Additives on the Carbonation of Reactive MgO Cements. *Cement Concrete Res.* 54, 87–97. doi:10.1016/j.cemconres.2013.08.009

Vandeperre, L. J., and Al-Tabbaa, A. (2007). Accelerated Carbonation of Reactive MgO Cements. *Adv. Cement Res.* 19, 67–79. doi:10.1680/adcr.2007.19.2.67

Vandeperre, L. J., Liska, M., and Al-Tabbaa, A. (2008). Hydration and Mechanical Properties of Magnesia, Pulverized Fuel Ash, and Portland Cement Blends. *J. Mater. Civil Eng.* 20, 375–383. doi:10.1061/(asce)0899-1561(2008)20:5(375)

Vu, M. H. (2012). *Effet des Contraintes et de la Température sur L'intégrité des Ciments des Puits Pétroliers*. Champs-sur-Marne, France: Theses, Université Paris-Est.

Walling, S. A., and Provis, J. L. (2016). A Discussion of the Papers "Impact of Hydrated Magnesium Carbonate Additives on the Carbonation of Reactive MgO Cements" and "Enhancing the Carbonation of MgO Cement Porous Blocks Through Improved Curing Conditions". *Cement Concrete Res.* 79, 424–426. doi:10.1016/j.cemconres.2015.09.010

Williams, H., Khatri, D., Keese, R., Le Roy-Delage, S., Roye, J., Leach, D., et al. (2011). "Flexible, Expanding Cement System (FECS) Successfully Provides Zonal Isolation across Marcellus Shale Gas Trends," in Canadian Unconventional Resources Conference, Calgary, Canada, 2011 (Calgary: Society of Petroleum Engineers), 2154–2172. doi:10.2118/149440-ms

Yang, Y., Deng, Y., and Li, X. (2019). Uniaxial Compression Mechanical Properties and Fracture Characteristics of Brucite Fiber Reinforced Cement-Based Composites. *Compos. Structures.* 212, 148–158. doi:10.1016/j.compstruct.2019.01.030

Ye, Q., Yu, K., and Zhang, Z. (2015). Expansion of Ordinary Portland Cement Paste Varied With Nano-MgO. *Construction Building Mater.* 78, 189–193. doi:10.1016/j.conbuildmat.2014.12.113

Zgueb, R., Brichni, A., and Yacoubi, N. (2018). Improvement of the Thermal Properties of Sorel Cements by Polyvinyl Acetate: Consequences on Physical and Mechanical Properties. *Energy and Buildings.* 169, 1–8. doi:10.1016/j.enbuild.2018.03.007

Zhang, D., Ghouleh, Z., and Shao, Y. (2017). Review on Carbonation Curing of Cement-Based Materials. *J. CO_2 Utilization.* 21, 119–131. doi:10.1016/j.jcou.2017.07.003

Zhang, R., Bassim, N., and Panesar, D. K. (2018). Characterization of Mg Components in Reactive MgO - Portland Cement Blends During Hydration and Carbonation. *J. CO_2 Utilization.* 27, 518–527. doi:10.1016/j.jcou.2018.08.025

Zhang, W., Hilgedick, S., and Eckert, A. (2019). *A Novel Approach to Investigate Cement Pore Pressure during HardeningAADE-19-NTCE-086.*

Zhang, W., Zheng, Q., Ashour, A., and Han, B. (2020). Self-Healing Cement Concrete Composites for Resilient Infrastructures: A Review. *Composites Part B: Eng.* 189, 107892. doi:10.1016/j.compositesb.2020.107892

Conflict of Interest: The authors declare that the research was conducted in the absence of any commercial or financial relationships that could be construed as a potential conflict of interest.

Publisher's Note: All claims expressed in this article are solely those of the authors and do not necessarily represent those of their affiliated organizations, or those of the publisher, the editors and the reviewers. Any product that may be evaluated in this article, or claim that may be made by its manufacturer, is not guaranteed or endorsed by the publisher.